Stockholm University

Bulk-boundary correspondence and biorthogonality in non-Hermitian systems

Elisabet Edvardsson

Doctoral Thesis in Theoretical Physics at Stockholm University, Sweden 2022

Bulk-boundary correspondence and biorthogonality in non-Hermitian systems

Elisabet Edvardsson

Academic dissertation for the Degree of Doctor of Philosophy in Theoretical Physics at Stockholm University to be publicly defended on Friday 20 January 2023 at 13.00 in Oskar Kleins auditorium (FR4), AlbaNova universitetscentrum, Roslagstullsbacken 21, and online via Zoom: https://stockholmuniversity.zoom.us/j/239996391.

Abstract

In topological insulators, the bulk-boundary correspondence describes the relationship between the bulk invariant -- computed for a system with periodic boundary conditions -- and the number of topological boundary states in the corresponding system with open boundary conditions. This is a well-known property of these systems and is important for predicting how they will behave. In recent years, however, the modeling of dissipative and non-equilibrium systems using non-Hermitian Hamiltonians has become increasingly popular. These systems feature many novel phenomena; in particular the bulk-boundary correspondence breaks down since the spectrum of the system with periodic boundary conditions typically differs fundamentally from the spectrum of the system with open boundary conditions.

In this thesis, the behavior of the boundary states in non-Hermitian lattice models is studied. The framework of biorthogonal quantum mechanics is used to develop the biorthogonal bulk-boundary correspondence, which predicts the (dis)appearance of the boundary states in these systems. Closely related to the drastic change in spectra between boundary conditions is the non-Hermitian skin effect. This refers to the exponential localization of almost all eigenstates to the boundaries and is typically seen in non-Hermitian lattice models. How to predict this, and how to quantify the sensitivity of the spectrum to the boundary conditions are therefore questions that are also studied in this thesis.

Keywords: *non-Hermiticity, bulk-boundary correspondence, biorthogonal quantum mechanics, skin effect.*

Stockholm 2022
http://urn.kb.se/resolve?urn=urn:nbn:se:su:diva-211890

ISBN 978-91-8014-118-5
ISBN 978-91-8014-119-2

Department of Physics

Stockholm University, 106 91 Stockholm

BULK-BOUNDARY CORRESPONDENCE AND BIORTHOGONALITY IN NON-HERMITIAN SYSTEMS

Elisabet Edvardsson

Stockholm
University

Bulk-boundary correspondence and biorthogonality in non-Hermitian systems

Elisabet Edvardsson

ISBN print 978-91-8014-118-5
ISBN PDF 978-91-8014-119-2

Printed in Sweden by Universitetsservice US-AB, Stockholm 2022

In loving memory of
Karl-Anders Edvardsson
and Svante Silvén.

Abstract

In topological insulators, the bulk-boundary correspondence describes the relationship between the bulk invariant – computed for a system with periodic boundary conditions – and the number of topological boundary states in the corresponding system with open boundary conditions. This is a well-known property of these systems and is important for predicting how they will behave. In recent years, however, the modeling of dissipative and non-equilibrium systems using non-Hermitian Hamiltonians has become increasingly popular. These systems feature many novel phenomena; in particular the bulk-boundary correspondence breaks down since the spectrum of the system with periodic boundary conditions typically differs fundamentally from the spectrum of the system with open boundary conditions.

In this thesis, the behavior of the boundary states in non-Hermitian lattice models is studied. The framework of biorthogonal quantum mechanics is used to develop the biorthogonal bulk-boundary correspondence, which predicts the (dis)appearance of the boundary states in these systems. Closely related to the drastic change in spectra between boundary conditions is the non-Hermitian skin effect. This refers to the exponential localization of almost all eigenstates to the boundaries and is typically seen in non-Hermitian lattice models. How to predict this, and how to quantify the sensitivity of the spectrum to the boundary conditions are therefore questions that are also studied in this thesis.

Sammanfattning

I topologiska isolatorer beskriver bulk-randkorrepondensen förhållandet mellan en bulkinvariant – som beräknas för ett system med periodiska randvillkor – och antalet topologiska kanttillstånd i motsvarande system med öppna randvillkor. Detta är ett välkänt förhållande hos sådana system och är viktigt för att förutsäga hur de ska bete sig. De senaste åren har det emellertid blivit populärt att modellera dissipativa system och icke-jämviktssystem med hjälp av icke-Hermiteska Hamiltonianer. I de systemen uppträder många nya fenomen. Framför allt bryter bulk-randkorrespondensen samman eftersom spektrumet för ett system med periodiska randvillkor skiljer sig fundamentalt från spektrumet för motsvarande system med öppna randvillkor.

I den här avhandlingen studeras beteendet hos kanttillstånd i icke-Hermiteska gittermodeller. Det ramverk som utgörs av biortogonal kvantmekanik används för att utveckla den biortogonala bulk-randkorresepondesen som förutsäger när kanttillstånd dyker upp och försvinner i systemet. Tätt sammankopplad med den stora förändringen i spektrum mellan öppna och periodiska randvillkor är den icke-Hermiteska skinneffekten. Med detta menas den exponentiella lokaliseringen till randen som typiskt ses hos nästan alla egentillstånd i icke-Hermiteska gittermodeller. Hur man förutsäger när detta inträffar och hur spektrumets känslighet för randvillkor kvantiseras, studeras därför också i den här avhandlingen.

Accompanying papers

PAPER I: Biorthogonal bulk-boundary correspondence in non-Hermitian systems
F. K. Kunst, E. Edvardsson, J. C. Budich, and E. J. Bergholtz (2018), Phys. Rev. Lett. 121, 026808

I researched the mathematical background, did computations that showed how quickly the spectrum changes when coupling the ends of the non-Hermtitian SSH-chain and contributed to the writing of the paper.

PAPER II: Non-Hermitian extensions of higher-order topological phases and their biorthogonal bulk-boundary correspondence
E. Edvardsson, F. K. Kunst, and E. J. Bergholtz (2019), Phys. Rev. B 99, 081302

I did most of the computations and plots and contributed to the writing of the paper.

PAPER III: Phase transitions and generalized biorthogonal polarization in non-Hermitian systems
E. Edvardsson, T. Yoshida, F. K. Kunst, E. J. Bergholtz (2020), Phys. Rev. Research 2, 043046

I did a big part of the detailed calculations together with F. K. Kunst and T. Yoshida, produced all plots and wrote the first draft.

PAPER IV: Sensitivity of non-Hermitian systems
E. Edvardsson, E. Ardonne (2022), Phys. Rev. B 106, 115107

I proposed the project, did parts of the analytical calculations for the one-dimensional systems, did most of the work on the two-dimensional systems and wrote most of the paper.

PAPER V: Biorthogonal renormalization
E. Edvardsson, J. L. K. König, M. Stålhammar (2022), Manuscript.

I proposed the project, worked together with the coauthors to develop a new inner product formalism and wrote big parts of the paper.

Additional paper by the author not included in the thesis:

The Q-toothpick cellular automaton
E. Edvardsson, E. Mossberg (2019), Journal of Cellular Automata 14

Material from my licentiate thesis

Parts of this dissertation overlap with the contents of my (unpublished) licentiate thesis [1]. Chapters 1, 2, 3.2 and 4.1-4.2.1 of this thesis have significant overlap with chapters 1, 2, 3.1 and 3.2, respectively, of [1].

Acknowledgements

First of all I would like to thank my supervisor Emil Bergholtz for suggesting successful projects as well as giving me the freedom to pursue work in other directions, for always having time to discuss physics, and for making me see physics from a different point of view. Many thanks also to my co-supervisor Eddy Ardonne for valuable guidance, for many interesting discussions and for sharing my interest in mathematical physics.

Furthermore, I would like to thank my other coauthors of the papers included in this thesis, Flore Kunst, Jan Budich, Tsuneya Yoshida, Marcus Stålhammar and Lukas König, for successful collaborations and for many interesting discussions and shared ideas.

Thanks also to my other colleagues at Stockholm University and elsewhere. In particular, I am grateful to Jonas Larson, Kang Yang and Fan Yang for all discussions about non-Hermitian physics. Thanks also to Sören Holst, Jürgen Fuchs and Marcus Berg for inspiring discussions about other areas of physics. Many thanks to Maria Hermanns, Peter Mogensen and Åsa Larson for useful comments on my thesis. A special thank you to Eva Mossberg for all discussions about mathematics and for good advice on teaching, LaTeX, and MATLAB.

Finally, I want to thank my friends and family for all their support. In particular, thanks to my parents for letting me use part of their basement as a home office during the pandemic, and to Napoleon the rabbit for being excellent lunch company during that time.

Contents

Chapter 1

Introduction

One of the main tasks of condensed matter physics is to classify different phases of matter. For a long time it was believed that all phase transitions could be understood in terms of symmetry breaking, like the transition from solid to liquid or between different crystal structures in a solid material. This is something Landau's theory of phase transitions explains. The foundation in this theory is the existence of a local order parameter.

However, in the past decades one has found several phases of matter that simply cannot be described in this way. Famous examples include the integer quantum Hall effect [2], which was discovered in 1980 and was the first example of such a phase, and the quantum spin Hall phase in graphene [3, 4], which was discovered in 2005. One important subset of systems whose phases are not fully described by Landau's theory consists of *topological insulators*, which include Chern insulators [5–7] and $\mathbb{Z}_2$ insulators [3, 4, 8–10]. A topological insulator is a bulk insulator for which one can compute a topological invariant from the bulk properties of the system. This invariant differentiates between the different phases the system can be in. In contrast to Landau's theory, there does not need to be any difference in symmetry between these phases. Typical for topological insulators is the presence of robust, gapless boundary states in the topological phase, that is the phase with a non-zero invariant. The invariant tells us the number of boundary states present in the system. This relationship is called the *bulk-boundary correspondence* and is of fundamental importance in this area of physics. The boundary states are furthermore either topologically protected or protected by some symmetry of the system and are thus robust as long as no 'violent' transformations are done to the system or as long as the symmetry persists.

More recent, but related, is the discovery of *higher-order topological insulators* [11–15]. Ordinary topological insulators are bulk insulators with d spatial dimensions that carry gapless boundary states on the $(d-1)$-dimensional boundaries. A

higher-order topological insulator, however, carries gapless boundary states on the $(d-n)$-dimensional boundaries.

In recent years, another branch of physics has gained momentum and become extremely popular to study, namely, that of systems described by non-Hermitian Hamiltonians. This is done both in classical settings, where the system is mapped to a Schrödinger-like equation, and in quantum settings. One of the fundamental postulates in quantum mechanics is the assumption that all observables are described by Hermitian operators. This implies e.g. reality of the eigenvalues and many other properties, both physically and mathematically. Non-Hermitian operators are typically more difficult to deal with. They can be very ill-conditioned in numerical settings, they are not necessarily diagonalizable and their left and right eigenvectors are typically not related by Hermitian conjugation. Physically, non-Hermiticity leads to several strange phenomena that at first glance seem unintuitive and hard to explain. Despite this, non-Hermitian Hamiltonians are useful to describe non-equilibrium systems, systems that feature gain or loss and systems that interact with the environment. It has turned out to be particularly useful in optical systems, where gain and loss needs to be implemented when light travels through a medium [16–26], but is also interesting in topoelectrical circuits [27–32] and mechanical systems [33–35]. It is, however, important to note that physics on a fundamental level always is Hermitian, but that one can use these non-Hermitian Hamiltonians to model for example quasiparticles or a non-isolated part of a larger system.

One topic that has gained a lot of attention is non-Hermtitian generalizations of topological systems. Such systems have been extensively studied in the past few years, both theoretically [36–49] and experimentally [50–60]. In the particular case of non-Hermitian generalizations of topological insulators, which is central to the accompanying papers of this thesis, the breakdown of the bulk-boundary correspondence [61–64] is of great importance. It turns out that the bulk energy spectrum differs significantly between systems with periodic and open boundary conditions, something that at first glance seems very unintuitive; if the boundary is very far away, you should not 'see' it from inside the bulk. This means that we can no longer immediately use the simple Bloch Hamiltonian to make predictions about the number of boundary states in the system.

The breakdown of the conventional bulk-boundary correspondence and how to find a new *biorthogonal bulk-boundary correspondence* is the main subject of the accompanying papers of this thesis. Since the bulk-boundary correspondence describes the relation between boundary states and bulk invariants, it is clear that it is important to understand the behavior of those boundary states in non-Hermitian systems. To accomplish this, we study a certain class of systems that are non-

Hermitian generalizations of Hermitian topological systems with exact solutions for the boundary states described in [65–67]. It turns out that the exact solutions generalize nicely to the non-Hermitian case, which gives way for a clear analysis. One important difference, however, is that the Hamiltonian, as previously mentioned, has left and right eigenstates that are not necessarily related by Hermitian conjugation. In order to account for that, we need to turn to the framework of biorthogonal quantum mechanics, described in [68], where one defines a new inner product that is used to compute quantum mechanical probabilities.

In Paper I, [69], *Biorthogonal bulk-boundary correspondence in non-Hermitian systems*, some one-dimensional non-Hermitian systems that have exact solutions are studied. Using the formalism of biorthogonal quantum mechanics, the gap closings and the existence of boundary states in the system are accurately predicted. Furthermore, the biorthogonal polarization is defined, which is an integer that takes the value 1 when there is a state at the boundary and 0 when there is not.

In Paper II, [70], *Non-Hermitian extensions of higher-order topological phases and their biorthogonal bulk-boundary correspondence*, non-Hermitian versions of higher-order topological insulators are studied. It is shown that the biorthogonal formalism can be used to understand the gap closings and boundary states in these models as well.

In Paper III, [71], *Phase transitions and generalized biorthogonal polarization in non-Hermitian systems*, properties of a generalization of the biorthogonal polarization introduced in [69] are discussed. Furthermore, results from Paper I are studied in more detail. In particular, it is proven that the gap closes at the predicted points. In addition to this, a method for finding not only the boundary states, but also all bulk states, is proposed.

In Paper IV, [72], *Sensitivity of non-Hermitian systems*, the sensitivity of the spectrum to boundary conditions is studied in more detail in one-dimensional systems. A method to find the eigenvalues of one-dimensional one-band models is described and applied to several systems in order to obtain analytical expressions for the eigenvalues, which enables quantifying the sensitivity of the spectrum. Furthermore, using these results, several two-dimensional systems are also studied.

Finally, in Paper V, [73], *Biorthogonal renormalization*, the biorthogonal inner product is studied in more detail. It is shown that the choice of scaling of the eigenvectors of the Hamiltonian can play a significant role when computing probabilities and expectation values. This means that one has to be very careful and make sure that what was done in Papers I-III is actually consistent, something which is proven in this work. An alternative inner product is defined, which makes comparisons between different systems easier, and the physical meaning of the

lattice sites in our lattice models is discussed.

This thesis aims at describing the background necessary to understand and appreciate the relevance of the accompanying papers. In Ch. 2, the relevant Hermitian systems that are generalized in the accompanying papers are introduced. We start with a short introduction to what a topological insulator is. Then we describe higher-order topological insulators and show how one uses the exact solutions mentioned to understand the behavior of the boundary states in a certain class of systems. Finally we have a short discussion about how to find the bulk states exactly in a special class of Hermitian systems. Ch. 3 concerns non-Hermitian systems. Here we illustrate the phenomena that can occur in such systems. In particular, we describe the skin effect and the extreme sensitivity of the spectrum to the boundary conditions. In Ch. 4, we give an introduction to biorthogonal quantum mechanics and the biorthogonal bulk-boundary correspondence and discuss how the degree of freedom in choosing the biorthogonal inner product affects the results. Finally, in Ch. 5, we provide a discussion and an outlook.

Chapter 2

Bulk-boundary correspondence in Hermitian systems

In order to understand and appreciate the non-Hermitian systems that are the focus of the accompanying papers, one first needs some background about the corresponding Hermitian systems. This chapter will not be a full review of those systems, but rather include the background necessary to understand the non-Hermitian generalizations we make.

2.1 Topology and boundary states

Topology (see e.g. [74]) is the part of mathematics where one studies the properties of sets that are preserved under what one can think of as continuous deformations. These deformations do not include for example gluing and cutting. More mathematically accurately, a topological property is preserved under maps that are called homeomorphisms. In physics, topology shows up in several different contexts, but in particular it is relevant in the study of phases in condensed matter systems. As mentioned in the introduction, topological phases are phases that cannot be described by the Landau theory of phase transitions, i.e. topological phases cannot be separated from each other by studying the symmetry of the system. Instead they differ from each other by some invariant that is usually related to a topological invariant that can be defined in the system. One should note that although many systems are called topological in this context, they might not all have an associated invariant that a mathematician would call topological.

2.1.1 Topological insulators

Topological insulators is a special class of systems in which topological phases exist. They are bulk insulators, which means that the system with periodic boundary conditions has a band gap, for which one can find a bulk invariant that differentiates between phases. This bulk invariant is related to the number of robust gapless boundary states – i.e. states that are insensitive to certain perturbations, are localized to the boundary of the system and have energies that lie in the band gap – present in the system[1]. When the bulk invariant is zero, we say that we are in the topologically trivial phase. This means that the system, in this phase, can be adiabatically transformed to the atomic limit, where the unit cells are completely disconnected from each other, without closing any gaps in the system. Transformation to, from and between topologically non-trivial phases requires a gap closing in the system. The relationship between a bulk invariant computed from a system with periodic boundary conditions and the number of gapless boundary states in the corresponding system with open boundary conditions, is called the *bulk-boundary correspondence* and is of great importance in this area of physics.

The first topological insulator discovered was the integer quantum Hall effect [2]. In this system the Hall conductance is quantized according to

$$\sigma_{xy} = \frac{e^2}{h} n, \tag{2.1}$$

where n is the Chern number and tells us the number of chiral edge states in the system. These edge states are topologically protected and are thus extremely robust to impurities and deformations of the system.

One class of topological insulators, which does not include the integer quantum Hall effect, consists of those that have symmetry protected boundary states. This means that as long as the particular symmetry of the system that protects these boundary states is present, the states will be robust. These systems might, naturally, be more sensitive to perturbations as those can break the symmetry. The fact that the boundary states are symmetry protected, enables a classification of topological insulators based on their symmetries. The most important symmetries in this context are time-reversal symmetry, charge conjugation symmetry and chiral symmetry, but in principle any discrete symmetry of the system could give rise to protected boundary states. These three symmetries, in particular, have given rise to a 'periodic table' of topological insulators, where a classification is made of which kind of invariant, $\mathbb{Z}$ or $\mathbb{Z}_2$, occurs in an n-dimensional system with specified symmetries [76, 77]. A $\mathbb{Z}_2$-invariant implies that there can exist either one or zero

[1] It seems like people do not entirely agree upon the definition of a topological insulator. Some, do not e.g. require the existence of the gapless boundary states [75].

gapless boundary states, while a $\mathbb{Z}$-invariant implies that there can be an integer number of them, as in the case of the integer quantum Hall effect where we have the Chern number.

Central to the above discussion is the existence of robust boundary states. The theory of topological insulators is well-known in the Hermitian case. The non-Hermitian case, however, is not so well-understood yet. One way to approach that subject is thus to examine the behavior of boundary states in non-Hermitian systems. This is what was done in Papers I-III. To appreciate and understand what was done there, the rest of this chapter will be devoted to the understanding of boundary states in Hermitian systems.

2.1.2 Tight-binding Hamiltonians

The integer quantum Hall effect mentioned above is a continuum system, but in this thesis we will be interested in lattice models. These, we will analyze in a tight-binding setting. In the tight-binding approximation, the Hamiltonian of a system with N sites, written in position basis, is given by

$$\mathcal{H} = \sum_{i,j=1}^{N} t_{ij} c_i^\dagger c_j = \mathbf{c}^\dagger H \mathbf{c}, \tag{2.2}$$

where $H = (t_{ij})$ is the matrix representation of the Hamiltonian, $c_i^\dagger$ creates an electron at site i and t_{ij} describes how easy it is for an electron to move from site i to site j. For now, we assume, as is standard in quantum mechanics, that the matrix H is Hermitian, i.e. that $t_{ij} = t_{ji}^*$. The parameters t_{ij} are referred to as *hopping parameters*.

This means that when analyzing the topological properties of systems, we are interested in the properties of the matrix H as a function of system parameters. In particular, we are interested in understanding the behavior of the eigenvalues and eigenvectors. Therefore, we will first make some general remarks about the tight-binding matrices that might show up. In general, the structure of the matrix depends on the dimension and the geometry of the system we are interested in, as well as the boundary conditions. There are, however, some general considerations that can be made.

One-dimensional systems.

A one-dimensional system can be described by the matrix

$$H_{1D} = \begin{pmatrix} A & B & & D^\dagger \\ B^\dagger & \ddots & \ddots & \\ & \ddots & \ddots & B \\ D & & B^\dagger & A \end{pmatrix}, \tag{2.3}$$

where A is a Hermitian matrix describing the unit cell, B describes the hopping between the unit cells and D describes the boundary conditions. Typically we are interested in systems with open or periodic boundary conditions in which cases we have $D = 0$ and $D = B$, respectively.

Two-dimensional systems.

We can easily use the above to extend our description to two-dimensional systems with rectangular geometry. By stacking one-dimensional chains, we get a two-dimensional system, whose Hamiltonian is of the form

$$H_{2D} = \begin{pmatrix} H_{1D} & B_2 & & D_2^\dagger \\ B_2^\dagger & \ddots & \ddots & \\ & \ddots & \ddots & B_2 \\ D_2 & & B_2^\dagger & H_{1D} \end{pmatrix}, \tag{2.4}$$

where H_{1D} is the matrix describing the one-dimensional systems, B_2 is the matrix describing the connection between them and D_2 the boundary conditions in the second direction.

Higher-dimensional systems.

It is clear that as long as we have a rectangular geometry, the procedure of describing an n-dimensional system as stacked $(n-1)$-dimensional systems using a block-Toeplitz matrix will work in any dimension, and we will have a matrix of the form

$$H_{nD} = \begin{pmatrix} H_{(n-1)D} & B_n & & D_n^\dagger \\ B_n^\dagger & \ddots & \ddots & \\ & \ddots & \ddots & B_n \\ D_n & & B_n^\dagger & H_{(n-1)D} \end{pmatrix}, \tag{2.5}$$

Therefore, understanding the behavior of block-tridiagonal block-Toplitz matrices is of importance to this.

Matrix perturbation theory.

In the next section, we will see an example of the bulk-boundary correspondence, but first, we will make a more general observation. Namely, inherent to the bulk-boundary correspondence is the fact that the bulk spectrum does not significantly change when we change the boundary conditions. That this is indeed the case, is suggested by a famous perturbation theorem for Hermitian matrices, called the Cauchy interlacing theorem, see e.g. [78]:

Theorem. Let A be a Hermitian $n \times n$-matrix with eigenvalues $\lambda_1 \geq \cdots \geq \lambda_n$ and let B be a principal submatrix of order $n-k$ of A with eigenvalues $\mu_1 \geq \cdots \geq \mu_{n-k}$. Then

$$\lambda_i \geq \mu_i \geq \lambda_{i+k}, \tag{2.6}$$

for $i = 1, 2, \ldots, n-k$.

This theorem means that if we remove a number of rows and a columns (with the same indices, respectively) of a Hermitian matrix, the remaining matrix will have eigenvalues that all lie in between the eigenvalues of the original matrix.

We know that the eigenvalues of the matrix

$$H_{nD} = \begin{pmatrix} H_{(n-1)D} & B_n & & B_n^\dagger \\ B_n^\dagger & \ddots & \ddots & \\ & \ddots & \ddots & B_n \\ B_n & & B_n^\dagger & H_{(n-1)D} \end{pmatrix}, \tag{2.7}$$

are given by the eigenvalues of the matrices

$$M = B_n^\dagger e^{-2\pi i k/N_1} + H_{(n-1)D} + B_n e^{2\pi i k/N_1}, \tag{2.8}$$

with $k = 0, \ldots, N_1 - 1$, where N_1 is the number of blocks on the diagonal. Since M is a Hermitian matrix and since $k/N_1 \in (-1, 1)$, the eigenvalues of $H_{(n-1)D}$ will be real and contained in a finite number of intervals, I_j. When the system is made larger, i.e. when the number of matrices $H_{(n-1)D}$ becomes larger, the eigenvalues will still be contained within the same intervals.

Suppose we have a matrix describing a periodic system and consider the principal submatrix constructed by removing the rows and columns containing the periodic boundary conditions. By the interlacing theorem, we know that the eigenvalues of the system with open boundary conditions will lie between the eigenvalues of the system with periodic boundary conditions. That is, almost all of them, will lie in the intervals I_j, but there might be a few isolated eigenvalues between these intervals. These are what we understand as boundary states.

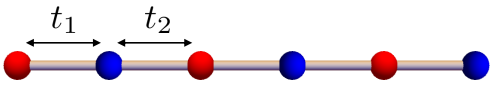

Figure 2.1: The SSH-chain.

This suggests that the bulk spectrum, i.e. the parts of the spectrum contained in the intervals I_j, is relatively insensitive to boundary conditions, which is one of the foundations for the bulk-boundary correspondence to work.

2.1.3 The SSH-chain

We now turn to the Su-Schrieffer-Heeger model, henceforth called the SSH-chain, which was introduced to describe solitons in a polyacetylene chain [79–81]. The SSH-chain has since become one of the most widely used systems to demonstrate and explain topological phenomena. The system is very simple, exactly solvable, and thus easy to analyze, but still demonstrates many important effects.

In Fig. 2.1, a sketch of the SSH-chain is shown. It consists of two different kinds of sites, A and B, inbetween which the electrons can move according to hopping amplitudes t_1 and t_2. The tight-binding Hamiltonian for the system with N unit cells is given by

$$\begin{aligned}\mathcal{H}_N &= \sum_{n=1}^{N}\left[t_1(c_{n,A}^\dagger c_{n,B} + c_{n,B}^\dagger c_{n,A})\right] + \sum_{n=1}^{N-1}\left[t_2(c_{n+1,A}^\dagger c_{n,B} + c_{n,B}^\dagger c_{n+1,A})\right] \\ &= \mathbf{c}^\dagger H_{\text{open},N}\mathbf{c},\end{aligned} \tag{2.9}$$

where $c_{n,i}^\dagger$ creates an electron in unit cell n at position i and $\mathbf{c}$ is a vector consisting of all creation operators. The matrix $H_{\text{open},N}$ is a $2N \times 2N$-matrix given by

$$H_{\text{open},N} = \begin{pmatrix} 0 & t_1 & & & & & \\ t_1 & 0 & t_2 & & & & \\ & t_2 & 0 & t_1 & & & \\ & & t_1 & 0 & \ddots & & \\ & & & \ddots & \ddots & t_1 & \\ & & & & t_1 & 0 \end{pmatrix}. \tag{2.10}$$

In a similar way, the Hamiltonian matrix for the corresponding system with periodic boundary conditions, that is the system where we have tied the two ends

together with a t_2 hopping, is given by the $2N \times 2N$-matrix

$$H_{\mathrm{per},N} = \begin{pmatrix} 0 & t_1 & & & & t_2 \\ t_1 & 0 & t_2 & & & \\ & t_2 & 0 & t_1 & & \\ & & t_1 & 0 & \ddots & \\ & & & \ddots & \ddots & t_1 \\ t_2 & & & & t_1 & 0 \end{pmatrix}. \tag{2.11}$$

Fourier transforming the system with periodic boundary conditions, we end up with the Bloch-Hamiltonian

$$H(k) = \begin{pmatrix} 0 & t_1 + t_2 e^{-ik} \\ t_1 + t_2 e^{ik} & 0 \end{pmatrix}, \tag{2.12}$$

which has eigenvalues

$$E_\pm(k) = \pm\sqrt{t_1^2 + t_2^2 + 2t_1 t_2 \cos(k)} \tag{2.13}$$

with corresponding unnormalized eigenvectors

$$\psi_{\mathrm{Bloch},\pm}(k) = \begin{pmatrix} t_1 + t_2 e^{-ik} \\ E_\pm(k) \end{pmatrix}, \tag{2.14}$$

where $k = 2\pi j/N$ and $j = 1, \ldots, N$. The spectrum of a periodic chain with $N = 40$ unit cells is shown in Fig. 2.2 as a function of t_1, together with the spectrum for the corresponding system with open boundary conditions.

We see in Fig. 2.2, that for $|t_1| < |t_2|$ we have two states with zero energy in the system. These are exponentially localized at different ends of the system, which can be seen by studying the corresponding eigenstates, so we have one boundary state at each end.

Now, let us see if we can find an invariant for this system. This is described in general particle-hole symmetric cases in [82]. The Bloch Hamiltonian can be written in the basis of Pauli matrices in the following way:

$$H(k) = \mathbf{d}(k) \cdot \sigma, \tag{2.15}$$

where σ is the vector of Pauli matrices, $\mathbf{d}(k) \in \mathbb{R}^3$ and $0 \leq k \leq 2\pi$. Explicitly, we have

$$d_x(k) = t_1 + t_2 \cos(k), \quad d_y(k) = t_2 \sin(k), \quad d_z(k) = 0, \tag{2.16}$$

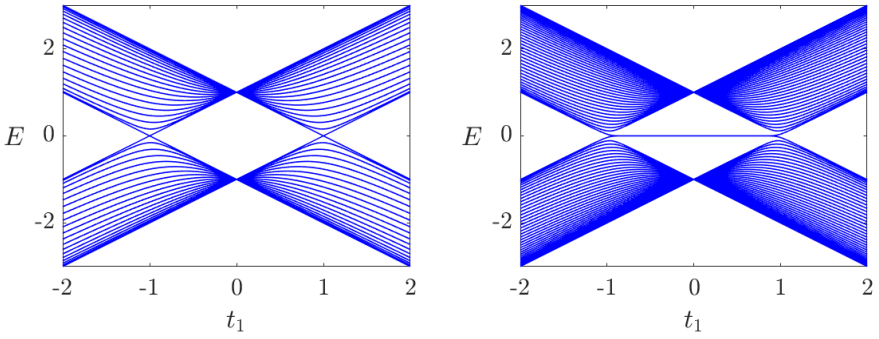

Figure 2.2: Spectrum for the SSH-chain with $t_2 = 1$ and $N = 40$ unit cells for the periodic (left) and open (right) systems. We see that the gap closes at $t_1 = \pm|t_2|$ and that we in the open system have two boundary states for $|t_1| < |t_2|$.

and we see that $\mathbf{d}(k)$ traces out a closed loop in the $d_x d_y$-plane as we change k from 0 to 2π. We can find the winding number of this loop around the origin, which is a homotopy invariant. The winding number is given by

$$\nu = \frac{1}{2\pi} \oint_C \frac{d_x \mathrm{d}(d_y) - d_y \mathrm{d}(d_x)}{d_x^2 + d_y^2}, \tag{2.17}$$

where C is the curve in the $d_x d_y$-plane traced out by $\mathbf{d}(k)$. Put differently, we have

$$\nu = \int_0^{2\pi} \frac{d_x(k) d_y'(k) - d_y(k) d_x'(k)}{d_x(k)^2 + d_y(k)^2} \mathrm{d}k = \frac{1}{2} + \frac{1}{4\pi} \int_0^{2\pi} \frac{t_2^2 - t_1^2}{t_1^2 + t_2^2 + 2t_1 t_2 \cos(k)} dk. \tag{2.18}$$

Evaluating the integral, we get

$$\nu = \begin{cases} 1 & \text{if } (t_1 - t_2)/(t_1 + t_2) > 0 \Leftrightarrow |t_1| > |t_2|, \\ 0 & \text{if } (t_1 - t_2)/(t_1 + t_2) < 0 \Leftrightarrow |t_1| < |t_2|, \end{cases} \tag{2.19}$$

and we see that the winding number is one exactly in the regions where we have a boundary state at each end and zero otherwise. This is an example of the bulk-boundary correspondence, and we see that one very nice feature is that we can use the Bloch Hamiltonian to compute the bulk invariant and use this number to predict the number of boundary states in the open system.

2.1.4 Higher-order topological insulators

So far we have discussed ordinary topological insulators. A d-dimensional topological insulator has an insulating bulk, but can host robust gapless boundary states

on the $(d-1)$-dimensional boundary of the system in the topological phase. However, in principle one could imagine that there can exist gapless boundary states on any boundary of dimension less than d. These systems are called *higher-order topological insulators* [83], and were initially explored by [11–15].

More precisely, we say that we have an nth order topological insulator if we have gapless boundary states on $(d-n)$-dimensional subsystems. In contrast to the toplogical insulators previously described, these states are not protected by topological invariants, but rather by spatial symmetries of the lattice. Furthermore, the states can depend on the shape of the surface.

2.2 Exact solutions for boundary states

Now, as previously mentioned, one of the key elements in the study of topological insulators is understanding the existence of boundary states in a system. In generic systems, there is no way to get exact expressions for them, since finding them requires diagonalization of big matrices, which in general cannot be done analytically. However, there exists a special class of systems that has been thoroughly described in [65–67] where one can find exact solutions for the boundary states. In what follows a description of such systems will be given.

In the special case that we will be considering, we have a d-dimensional lattice, described by the Hamiltonian H, with open boundary conditions in $d-n$ dimensions that is built up from the sublattices $A, B_1, B_2, \ldots, B_{d-n}$. The lattice is then created by stacking alternating A and B_i sublattices in the ith direction, such that we have A-sublattices at all boundaries. The hoppings on these lattices are restricted by the fact that we do not allow hoppings between A-sublattices. The SSH-chain with a broken unit cell at one end and the systems shown in Figs. 2.4 and 2.5 are some examples of systems that are of this form.

Let h_A be the Hamiltonian describing the lattice A and let n_A denote the number of sites in this lattice. The operator h_A will then have n_A eigenvalues that we denote by $E_{A,i}$. It now turns out that $E_{A,i}$ is also an eigenvalue of H and that the corresponding eigenstate of H is a state with zero amplitude on all B_i-lattices given by

$$|\psi_i\rangle = \mathcal{N}_i \sum_{\mathbf{m}_s} \prod_{q=1}^{d-n} r_{i,q}^{m_{s,q}} c^\dagger_{A,i,\mathbf{m}_s} |0\rangle \,. \tag{2.20}$$

Here i labels the state, $\mathcal{N}_i$ is a normalization factor, m_s labels the A lattices in the s-direction, $c^\dagger_{A,i,\mathbf{m}_s}$ creates an electron with energy $E_{A,i}$ in the A sublattice in the unit cell labelled by $\mathbf{m}_s = (m_{s,1}, \ldots, m_{s,d-n})$, and $r_{i,q}$ is a number that can be

determined from a simple equation resulting from the fact that the state has zero amplitude on all the B_i sites.

We note that these solutions have a very special form. Namely, assuming that $n_A = 1$, the probability of finding a particle described by such a state at an A-site is given by

$$P_A(\mathbf{m}_s) = |\mathcal{N}|^2 \prod_{q=1}^{d-n} |r_q|^{2m_{s,q}}, \tag{2.21}$$

and at a B_j-lattice site by

$$P_{B_j}(\mathbf{m}_s) = 0. \tag{2.22}$$

That is, we see that if some of the $|r_{i,q}| \neq 1$, the state will be exponentially localized to some boundaries of the system. On the other hand, if all $|r_{i,q}| = 1$, the state will be completely delocalized in the lattice, and thus be a bulk state. At this point, there should therefore also be a gap closing in the system, as this is where the boundary state becomes a bulk state. This means that if we can write $r_{i,q}$ in terms of parameters of the system, we can predict the existence of boundary states under adiabatic deformation of the system.

The probabilities for finding the particle at different sites can also be thought of as expectation values of the projection operator

$$\Pi_{\mathbf{m}_s} = |e_{\mathbf{m}_s}\rangle \langle e_{\mathbf{m}_s}|, \tag{2.23}$$

that projects onto unit cell $\mathbf{m}_s$. (Note that since the lattice has A-sites at all boundaries, it necessarily must contain broken unit cells. For those broken unit cells the projection is onto those sites in the unit cell that are actually there.) This observation will be of use in the non-Hermitian case that we will describe in Ch. 4.

We will now turn to some concrete examples to see how this can be used to obtain important information about the boundary states in a system.

2.2.1 The SSH-chain

Returning to the SSH-chain that was described in Sec. 2.1.3, we note that if we remove the last site in the chain, we have a boundary state of the form described in Eq. (2.20). In this case it is given by

$$|\psi\rangle = \mathcal{N} \sum_{m=1}^{N} r^m c^\dagger_{A,m} |0\rangle, \tag{2.24}$$

where $r = -t_1/t_2$. This state has corresponding eigenvalue $E = 0$ for all values of t_1 and t_2. The existence of this eigenvalue can be seen in Fig. 2.3, where the

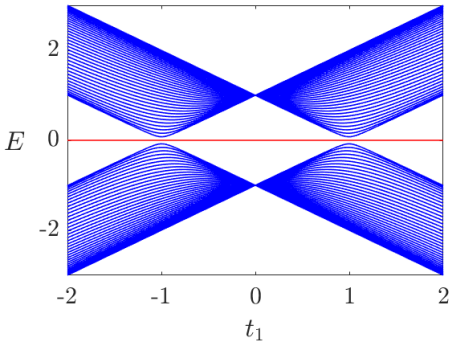

Figure 2.3: Plot of the energy eigenvalues for the SSH-chain with a broken unit cell for $t_2 = 1$ and $N = 40$. We see that we have one exact zero eigenvalue for all values of t_1.

spectrum is plotted for different values of t_1. The normalization constant is given by

$$\mathcal{N} = \frac{1}{r}\sqrt{\frac{1-r^2}{1-r^{2N}}}. \tag{2.25}$$

We see that depending on the relative sizes of t_1 and t_2, the state in Eq. (2.24) will either be localized to one of the edges of the chain or completely delocalized. More precisely, we see that for $|t_1| < |t_2|$, the state will be localized to the end of the chain where $m = 1$ and for $|t_1| > |t_2|$ to the end where $m = N$. For $|t_1| = |t_2|$, the point where the state changes its localization, it becomes completely delocalized in the chain. This also implies that the gap should close in the system, which we indeed see happens in Fig. 2.3.

Now we can use the knowledge of the localization of this zero mode to predict what happens in the system with unbroken unit cell. The gap closings and zero modes in the SSH-chain are defined in the thermodynamic limit, i.e. when we let $N \to \infty$. The Hamiltonian for the SSH-chain with a broken unit cell can be represented by the $(2N-1) \times (2N-1)$-matrix

$$H_{\text{broken},N} = \begin{pmatrix} 0 & t_1 & & & & \\ t_1 & 0 & t_2 & & & \\ & t_2 & 0 & t_1 & & \\ & & t_1 & 0 & \ddots & \\ & & & \ddots & \ddots & t_2 \\ & & & & t_2 & 0 \end{pmatrix}, \tag{2.26}$$

where N is the number of unit cells. The zero state is given by

$$\psi_{\text{exact},N} = \mathcal{N} \begin{pmatrix} r \\ 0 \\ r^2 \\ 0 \\ r^3 \\ \vdots \\ r^N \end{pmatrix}. \tag{2.27}$$

Now, let

$$\psi_{1,N} = \begin{pmatrix} \psi_{\text{exact},N} \\ 0 \end{pmatrix} = \begin{pmatrix} r \\ 0 \\ r^2 \\ 0 \\ r^3 \\ \vdots \\ r^N \\ 0 \end{pmatrix} \quad \text{and} \quad \psi_{2,N} = \begin{pmatrix} 0 \\ r^N \\ 0 \\ r^{N-1} \\ \vdots \\ r^2 \\ 0 \\ r^1 \end{pmatrix}. \tag{2.28}$$

Going back to the SSH-chain with unbroken unit cells defined in Eq. (2.10), we see that

$$H_{\text{open},N}\psi_{1,N} = \begin{pmatrix} 0 & t_1 & & & & \\ t_1 & 0 & t_2 & & & \\ & t_2 & 0 & t_1 & & \\ & & t_1 & 0 & \ddots & \\ & & & \ddots & \ddots & t_1 \\ & & & & t_1 & 0 \end{pmatrix} \begin{pmatrix} r \\ 0 \\ r^2 \\ 0 \\ r^3 \\ \vdots \\ r^N \\ 0 \end{pmatrix} = \begin{pmatrix} 0 \\ 0 \\ \vdots \\ 0 \\ t_1 r^N \end{pmatrix} \tag{2.29}$$

Expressed differently and considering all states as part of an infinite-dimensional Hilbert space on which the Hamiltonians $\mathcal{H}_N$ act, we have for $|r| < 1$

$$\lim_{N\to\infty} \mathcal{H}_N |\psi_{1,N}\rangle = \lim_{N\to\infty} t_1 r^N c^\dagger_{B,N} |0\rangle = 0, \tag{2.30}$$

We thus see that if $|r| < 1$, then in the limit, $|\psi_{1,N}\rangle$ becomes an eigenstate with eigenvalue 0. In a similar fashion, we also see that in the limit, $|\psi_{2,N}\rangle$ must also

be an eigenstate with zero eigenvalue for $|r| < 1$. That is, for $|r| < 1$, we have one boundary state at each end of the chain. We note, however, that for $|r| > 1$, these are not eigenstates. One can also argue that there can be no boundary states at all in this case. Namely, one can show (which we will do in Sec. 2.3), that apart from the exact state Eq. (2.24) in the SSH-chain with a broken unit cell, there are no other boundary states. Using a very similar argument to what was just done, one can show that one has an exponentially localized boundary state in the SSH-chain with broken unit cell at end $m = 1$ if and only if one has an exponentially localized boundary state at both ends in the SSH-chain with unbroken unit cells. This means that we do not have any boundary states for $|r| > 1$.

We can understand this physically. If we compare the even and odd chains, they should display the same physics at the $m = 1$ end of the chain for large systems, since the other end ends up very far away. That is, when we have the exact zero state localized at the $m = 1$ end in the chain, which happens when $|r| < 1$, with the broken unit cell, it should exist in the corresponding unbroken chain also. But the unbroken chain is mirror symmetric and has two ends that are equivalent, which means that there must be one boundary state at each end of the chain. Similarly, we do not have a boundary state at the $m = 1$ end for $|r| > 1$, which means that we should have no boundary state at all for these parameter values. What all of this means is that we can use the localization of the exact boundary states in the broken chain to predict when we have boundary states in the unbroken chain, and since they have an exact form for all system sizes this simplifies the analysis.

2.2.2 The Kagome lattice

Next, we turn to the Kagome lattice, which exhibits higher-order boundary states. It is built up from a net of SSH-chains, and can be analyzed in the same way as described earlier. Fig. 2.4 shows the rhombic and triangular Kagome lattices. We note that the triangular one has complete unit cells, while the rhombic one fits the description of a system with exact boundary states. In the same way as was just shown for the SSH-chain, we will thus use the exact solutions of the rhombic system to try to understand the triangular system [65].

The rhombic Kagome lattice has the following exact solution for the state with zero energy:

$$|\psi\rangle = \mathcal{N} \sum_{m_1=1}^{N} \sum_{m_2=1}^{N} r_1^{m_1} r_2^{m_2} c^\dagger_{A,m_1,m_2} |0\rangle \,, \tag{2.31}$$

where $r_1 = -t_1/t_2$, $r_2 = -t_1/t_2$, $c^\dagger_{A,m_1,m_2}$ creates an electron at the A sublattice in unit cell (m_1, m_2), $\mathcal{N}$ is a normalization constant and N is the number of unit cells in each direction. We see that since $r_1 = r_2$, the state must be localized either to

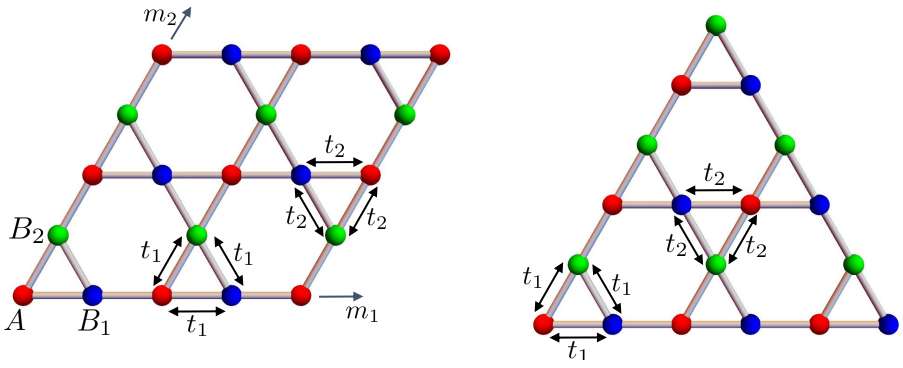

Figure 2.4: The rhombic and the triangular Kagome lattices.

the $(1,1)$ or the (m,m) corner and when it changes localization at $|r_1| = |r_2| = 1$ it does so by delocalizing completely in the whole bulk.

So what does this mean for the triangular system? We note that in the large system limit the $(1,1)$ corner in the rhombus locally behaves like the corners in the triangular lattice. This means that for $|r_1| = |r_2| < 1$ we have one corner state with zero energy eigenvalue in each corner, and thus in the large system size limit, we get a three-fold degenerate zero energy.

2.2.3 Chiral hinge states

The final model we will discuss in this section is one where we can find chiral hinge states. This model consists of stacked Rice-Mele chains as in Fig. 2.5 and was described in [65].

In practice, the t-dependence of the hoppings means that we can interpret the model as three-dimensional, where the third dimension is continuous and has momentum labeled by t. For each value of t, we have the following expression for a chiral hinge state with energy $-\sin(t)$

$$|\psi\rangle = \mathcal{N} \sum_{m_1=1}^{N} \sum_{m_2=1}^{N} r_1^{m_1} r_2^{m_2} c^\dagger_{A,m_1,m_2} |0\rangle \,, \tag{2.32}$$

where $r_1 = -(-t_1 + \delta\cos(t))/(-t_1 - \delta\cos(t))$ and $r_2 = -1$ and N is the number of unit cells in each direction. It is thus completely delocalized in the m_2-direction and exponentially localized to one of the sides in the m_1-direction. This means that if we go through the values of t, we will get a boundary state that is localized at one of the hinges. This state will switch hinge when $|r_1| = 1$, since this is when

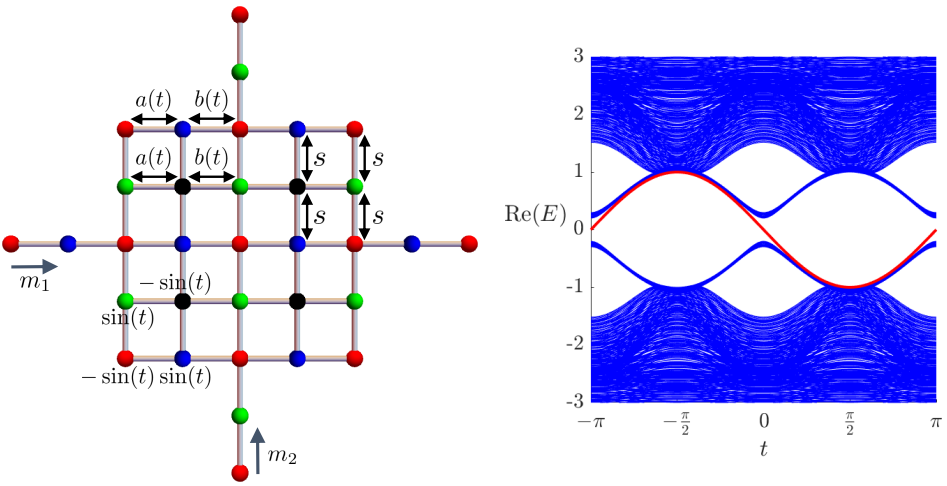

Figure 2.5: Left: Schematic picture of the model built up by Rice-Mele chains. The hoppings in the chains are given by $a(t) = -t_1 + \delta\cos(t)$ and $b(t) = -t_1 - \delta\cos(t)$. Right: Energy spectrum for the model for $t_1 = 1.5$, $\delta = 1$, $s = 0.25$ and $N = 10$. The chiral hinge state is depicted in red and we see that it attaches to the bulk at $t = \pm\pi/2$.

it delocalizes completely in the m_1-direction. That is, it happens when

$$|r_1| = \left| -\frac{-t_1 + \delta\cos(t)}{-t_1 - \delta\cos(t)} \right| = 1, \tag{2.33}$$

which implies that $t = \pm\pi/2$. These are also the points where the state changes chirality. The spectrum as a function of t is plotted in Fig. 2.5. We see that the t-values given by Eq. (2.33) correspond to points in the spectrum where the chiral hinge state (in red) attaches to the rest of the spectrum. The part of the spectrum plotted in blue consists of two different parts; we see both the bulk states and the surface states.

2.3 Finding all bulk states

Up until now, we have had our main focus on the boundary states, but to prove that the gap closes at the predicted points, and to know that the boundary states we have found are the only ones, one needs knowledge about the bulk states also. Finding analytic expressions for bulk states is easy to do in a periodic system, as the Bloch Hamiltonian for systems with small unit cells is easy to diagonalize exactly, even for large systems. On the other hand, the problem is much harder to solve for the system with open boundary conditions. In [84] a procedure for finding the bulk states in a family of such systems is described and we will now give a description of this procedure as we generalize it to the non-Hermitian case in Paper III.

Consider a d-dimensional system consisting of alternating $(d-1)$-dimensional A and B lattices, with open boundary conditions in one direction, and with the property that the corresponding Bloch Hamiltonian has energy eigenvalues that satisfy

$$E(\mathbf{k}) = E(-\mathbf{k}). \tag{2.34}$$

Furthermore, we assume that the A-lattices have n degrees of freedom, that the B-lattices have one degree of freedom, and that the electrons cannot hop directly between A-sites. This, for example, includes the SSH-chain with a broken unit cell. To simplify notation, we will only show the method for the SSH-chain here, but all calculations can be straightforwardly generalized to all the systems in this family.

Consider a periodic SSH-chain with $2M$ unit cells, as in Fig. 2.6. Let us denote

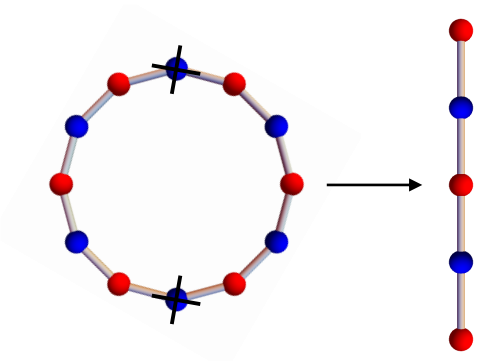

Figure 2.6: Assuming zero amplitude on the crossed-over sites in the periodic system gives us two completely detached SSH-chains with broken unit cells.

the eigenvectors of the Bloch Hamiltonian in Eq. (2.14), by

$$\psi_{\text{Bloch},\pm}(k) = \begin{pmatrix} \psi_{A,\pm}(k) \\ \psi_{B,\pm}(k) \end{pmatrix}, \tag{2.35}$$

where

$$\psi_{A,\pm}(k) = t_1 + t_2 e^{-ik}, \quad \psi_{B,\pm}(k) = \pm E(k), \tag{2.36}$$

for $k = j\pi/M$ and $j = 1, \ldots, 2M$. The corresponding real space eigenvector is now given by

$$\psi_{RS,\pm}(k) = \begin{pmatrix} e^{ik}\psi_{\text{Bloch},\pm}(k) \\ e^{2ik}\psi_{\text{Bloch},\pm}(k) \\ \vdots \\ e^{2Mik}\psi_{\text{Bloch},\pm}(k) \end{pmatrix}. \tag{2.37}$$

Denote by $\psi_{\text{Bulk},i,\pm}(k,m) = e^{ikm}\psi_{i,\pm}(k)$ the new bulk state at site $i \in \{A, B\}$ in the mth unit cell, such that

$$\psi_{RS,\pm}(k) = \begin{pmatrix} \psi_{\text{Bulk},A,\pm}(k,1) \\ \psi_{\text{Bulk},B,\pm}(k,1) \\ \psi_{\text{Bulk},A,\pm}(k,2) \\ \psi_{\text{Bulk},B,\pm}(k,2) \\ \vdots \\ \psi_{\text{Bulk},A,\pm}(k,M) \end{pmatrix}. \tag{2.38}$$

Now, since we know that $E(k) = E(-k)$ for the SSH-chain, the vectors $\psi_{RS,\pm}(k)$ and $\psi_{RS,\pm}(-k)$ must have the same energy. That is, any linear combination of

these two vectors must also be an eigenvector of the Hamiltonian. This means that

$$\begin{aligned}\psi_{\text{Bulk},i}(k,m) &= \mathcal{A}\psi_{i,\pm}(k,m) + \mathcal{B}\psi_{i,\pm}(-k,m) \\ &= \mathcal{A}e^{ikm}\psi_{i,\pm}(k) + \mathcal{B}e^{-ikm}\psi_{i,\pm}(-k).\end{aligned} \tag{2.39}$$

Now, if we impose the condition that

$$\psi_{\text{Bulk},B,\pm}(k,2M) = \psi_{\text{Bulk},B,\pm}(k,M) = 0, \tag{2.40}$$

for all k, we see that we get two SSH-chains with broken unit cells that are completely detached from each other. This is illustrated in Fig. 2.6. This condition implies

$$\frac{\mathcal{B}}{\mathcal{A}} = -\frac{\psi_{B,\pm}(k)}{\psi_{B,\pm}(-k)} = -\frac{\pm E(k)}{\pm E(-k)} = -1, \tag{2.41}$$

which means

$$\psi_{\text{Bulk},i,\pm}(k,m) = e^{ikm}\psi_{i,\pm}(k) - e^{-ikm}\psi_{i,\pm}(-k), \tag{2.42}$$

or more explicitly

$$\begin{aligned}\psi_{\text{Bulk},A,\pm}(k,m) &= e^{ikm}(t_1 + t_2e^{-ik}) - e^{-\mathrm{i}km}(t_1 + t_2e^{ik}) \\ &= 2i\left[t_1\sin(km) + t_2\sin(k(m-1))\right],\end{aligned} \tag{2.43}$$

and

$$\psi_{\text{Bulk},B,\pm}(k,m) = e^{ikm}E_{\pm}(k) - e^{-ikm}E_{\pm}(-k) = 2iE_{\pm}(k)\sin(km). \tag{2.44}$$

This means that Eq. (2.38), together with Eqs. (2.43) and (2.44), must form eigenvectors for the SSH-chain with M unit cells with the last unit cell broken. For $k = j\pi/M$ and $j = 1,\ldots,M-1$, we note that they are also orthogonal to each other, which, together with the exact solution described in Sec. 2.2, gives us $2M-1$ states in total, which is precisely the number eigenstates of the Hamiltonian.

By analyzing the expression for these states, we see that all of them are delocalized in the bulk, so all of them correspond to bulk states. Since the Hamiltonian is Hermitian, extension of the system by one site with hoppings comparable to hoppings in the rest of the system, should not be able to turn all these bulk states into non-bulk states as this would require them to change exponentially. This means that even though we have found these bulk states in the system with a broken unit cell, we can conclude that we must have at least this number of bulk states also in the system with complete unit cells. There will then be two states remaining to analyze, and those are precisely the ones given by $|\psi_{1,N}\rangle$ and $|\psi_{2,N}\rangle$.

Chapter 3

Non-Hermitian systems

In this chapter an introduction to non-Hermitian systems will be given. We will talk about Hamiltonians since we will solve Schrödinger-like equations with non-Hermitian Hamiltonians, but as we will see the applications are so far mainly not in quantum mechanics.

3.1 What is a non-Hermitian system?

To appreciate the difficulty with non-Hermitian systems, it is important to first be aware of how special Hermitian operators are, so here we collect some of the main properties of Hermitian operators. Let $\mathcal{H}$ be a Hilbert space and let $Q : \mathcal{H} \to \mathcal{H}$ be a Hermitian operator. Then the following is true.

1. The eigenvalues of Q are real.
2. Eigenvectors belonging to different eigenvalues are orthogonal to each other.
3. Q is unitarily diagonalizable, meaning that the eigenvectors form a complete basis for $\mathcal{H}$ and that if $|q\rangle$ is a right eigenvector of Q with eigenvalue q, then $\langle q|$ is a left eigenvector of Q with eigenvalue q.
4. The expectation value $\dfrac{\langle\alpha|Q|\alpha\rangle}{\langle\alpha|\alpha\rangle}$ is real for all $|\alpha\rangle \in \mathcal{H}$.

In particular the first and the fourth of these statements are reasons for us using Hermitian operators to describe observables in quantum mechanics – since the eigenvalues are tied to measurement outcomes, we want them to be real.

Letting go of the Hermiticity condition would mean that at least one of these statements is no longer true, which is potentially problematic from a physics point of view and something that needs to be carefully considered. We do, however,

note that some of the statements may still be true. For example, we can have a non-Hermitian matrix with real eigenvalues. This is the case for PT-symmetric systems that have been extensively studied in e.g. [85–88]. Non-Hermitian systems, however, became really popular when people started to let go of the reality condition and allow for complex eigenvalues. So far the applications have mainly been in classical systems, where non-Hermiticity is easier to implement. Examples of these systems include e.g. mechanical systems [34, 35, 89], photonic systems [16–26] and topoelectrical circuits [27–30]. While non-Hermiticity naturally shows up in optical systems in the form of gain an loss, the idea in other kinds of systems is that e.g. the equations of motions of mechanical systems or linearized wave equations can be rewritten in a Schrödinger-equation like form,

$$i\frac{d}{dt}\mathbf{x} = H\mathbf{x}, \tag{3.1}$$

where H is a matrix and $\mathbf{x}$ corresponds to a vector of some physical quantities, or transformations of such, in the system. This is what has been done in e.g. [35], where the idea is based on similar mappings made in the Hermitian case. In this particular case of a mechanical system, the vector $\mathbf{x}$ contains positions and velocities.

All of this concerns classical physics, but it is natural to also look for implementations in the quantum regime. Here the experimental results are fewer, but there are several suggestions of what to study. Most notably, we have the Lindblad equation [90], which describes interactions between a system described by the (Hermitian) Hamiltonian H_0 and the environment via a set of Lindblad operators L_n. The Lindblad equation is given by

$$\frac{d}{dt}\rho = \frac{\hbar}{i}\left[H_0, \rho\right] + \sum_n \left[L_n \rho L_n^\dagger - \frac{1}{2}\left(L_n^\dagger L_n \rho + \rho L_n^\dagger L_n\right)\right], \tag{3.2}$$

where ρ is the density matrix of the system. We note that non-Hermiticity comes into play in (at least) two ways here. First of all, the right-hand side can be described in terms of a Liouvillian super operator, such that

$$\frac{d}{dt}\rho = \mathcal{L}(\rho), \tag{3.3}$$

where $\mathcal{L}$ is a linear operator. Representing ρ as a vector, we can represent $\mathcal{L}$ as a matrix, which typically will be non-Hermitian. Thus non-Hermitian operators are relevant for understanding the Lindblad equation. This is studied in e.g. [91, 92], where, in particular, the damping matrix is of interest. In [92] it is shown that the Liouvillian for certain dissipative fermionic chains can be diagonalized by a

non-Hermitian matrix H_S, which in the case considered has the structure of a non-Hermitian SSH-chain (see Sec. 3.2). The matrix H_S is related to the damping matrix, which means that properties of the non-Hermitian matrix H_S, such as the skin effect, then carry over to the quantum system.

Secondly, there is also another non-Hermitian operator that can be extracted from the Lindblad equation. This can be seen by noting that the Lindblad equation can be simulated using a Monte Carlo method. In these settings, it turns out that it is the term $L_n \rho L_n^\dagger$ that is responsible for the so called quantum jumps, which switch trajectory in the simulation. This means that in order to understand the time evolution of ρ in very short time-frames or if we are only interested in a specific trajectory in the simulation, we can neglect this term. Then it turns out that the Lindblad equation can be rewritten as a Schrödinger equation with an effective Hamiltonian, H_{eff}, given by

$$H_{\text{eff}} = H_0 - \frac{i}{2} \sum_n L_n^\dagger L_n. \tag{3.4}$$

This is also studied in [92], where in the same kinds of systems where H_S had the structure of an SSH-chain, also H_{eff} has the same structure.

In conclusion, non-Hermitian operators are useful in many different contexts. In what follows, we will study the properties of non-Hermitian lattice models, where the Hamiltonian resembles what we would call a tight-binding Hamiltonian in the Hermitian case. In such systems, non-Hermiticity can be implemented either by adding an imaginary potential to each site or by making the hopping asymmetric.

3.2 Breakdown of the bulk-boundary correspondence

In this section, we will illustrate in more detail some of the effects that can occur if we let go of the Hermiticity condition. For simplicity, we keep the discussion to the SSH-chain with asymmetric hopping, which e.g. has been described in [93], but these phenomena occur also in other, more complicated systems.

We add a $\pm\gamma$-term to the t_1-hoppings described in Sec. 2.1.3. The resulting model is illustrated in Fig. 3.1. The Bloch Hamiltonian for this system is given by

$$H_{\text{Bloch}}(k) = \begin{pmatrix} 0 & t_1 + \gamma + t_2 e^{-ik} \\ t_1 - \gamma + t_2 e^{ik} & 0 \end{pmatrix}, \tag{3.5}$$

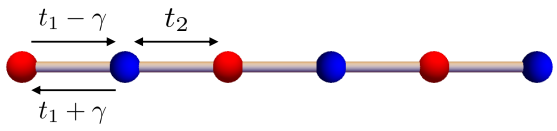

Figure 3.1: A non-Hermitian SSH-chain with asymmetric hoppings.

and the Hamiltonian for the open system by

$$\begin{aligned}\mathcal{H}_{\text{open}} = &\sum_{n=1}^{N}\left[(t_1+\gamma)c_{n,A}^{\dagger}c_{n,B} + (t_1-\gamma)c_{n,B}^{\dagger}c_{n,A}\right] \\ &+ \sum_{n=1}^{N-1}\left[t_2(c_{n+1,A}^{\dagger}c_{n,B} + c_{n,B}^{\dagger}c_{n+1,A})\right],\end{aligned} \tag{3.6}$$

which on matrix form gives us

$$H = \begin{pmatrix} 0 & t_1-\gamma & & & \\ t_1+\gamma & \ddots & t_2 & & \\ & t_2 & \ddots & \ddots & \\ & & \ddots & \ddots & t_1-\gamma \\ & & & t_1+\gamma & 0 \end{pmatrix} \tag{3.7}$$

Diagonalizing the Hamiltonian for both open and periodic boundary conditions, we note several things. First of all, the eigenvalues are not real. This means that – apart from having to figure out what complex energies mean – it is not as straightforward to define gap closings as in the Hermitian case, which is problematic if we want to predict the (dis)appearence of boundary states. In this particular case, however, one can show that the boundary state that we are interested in modeling has eigenvalue zero for all parameter values that it exists for. This means that a gap closing which can cause the edge state to disappear should mean that there is a gap closing at zero energy in the absolute value spectrum. In more general cases, one can talk about line gaps and point gaps [43]. These will be discussed in more detail in the next section since it turns out that there are important differences between these kinds of gap closings.

In Fig. 3.2, we plot the absolute value of the spectra for the non-Hermitian SSH-chains with periodic and open boundary conditions, respectively, as a function of t_1. As was noted in [62, 93], we see that the bulk spectra are vastly different and that the gap closings occur at very different parameter values. This means

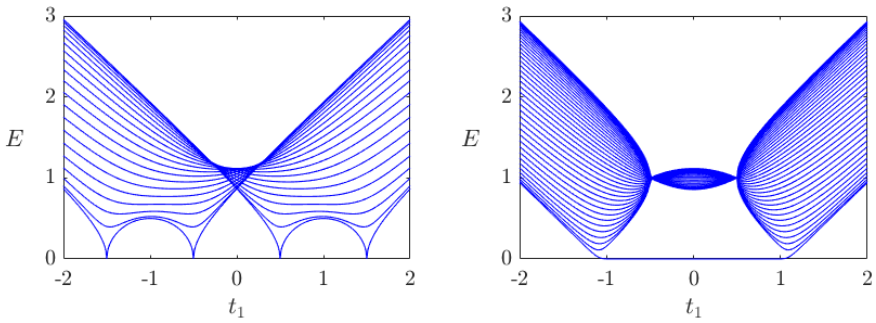

Figure 3.2: The absolute value of the energy eigenvalues for the non-Hermitian SSH-chain at $t_2 = 1$ and $\gamma = 0.5$ for $N = 40$ unit cells for periodic (left) and open (right) boundary conditions.

that the bulk-boundary correspondence we take for granted in Hermitian systems apparently must fail here. If the gap closings in the periodic spectrum do not correspond to the gap closings in the open system, they cannot be used to predict phase transitions or a change in the number of boundary states. This is because we expect, just as in the Hermitian case, that these only can occur at the gap closings. The fact that we get this difference between the spectra is seemingly counterintuitive, since it means that no matter how large the system is, a tiny change at one point in the lattice will still significantly affect the bulk spectrum. In Sec. 3.3, we will look at why this is the case.

Another property of non-Hermitian operators is that they are not necessarily diagonalizable. In this case, this happens in the system with open boundary conditions at $t_1 = \pm\gamma$. At first glance these points might look as points where the states are highly degenerate. Upon closer inspection, however, it turns out that we do not have a complete set of eigenstates for the Hamiltonian here. Such points are called exceptional points and contain a lot of interesting physics [21, 45, 94, 95].

We can also study the states explicitly. In Fig. 3.3, we plot the absolute value of the eigenvectors of the SSH-chain for $t_1 = 0.8$, $\gamma = 0.5$, $t_2 = 1$. We see that all eigenstates are exponentially localized to the boundaries. This is an example of the so called *skin effect* [63, 64, 93], which we will discuss in more detail in next section. At first glance, this localization might seem unintuitive, but the reason for it can be understood by the fact that we have the asymmetry which drives towards one of the ends of the chain and thus creates this build up. It also fits well with the big difference between the spectra of the systems with periodic and open boundary conditions respectively; because of this localization, the spectrum is exponentially sensitive to coupling between the ends as there is no end to localize

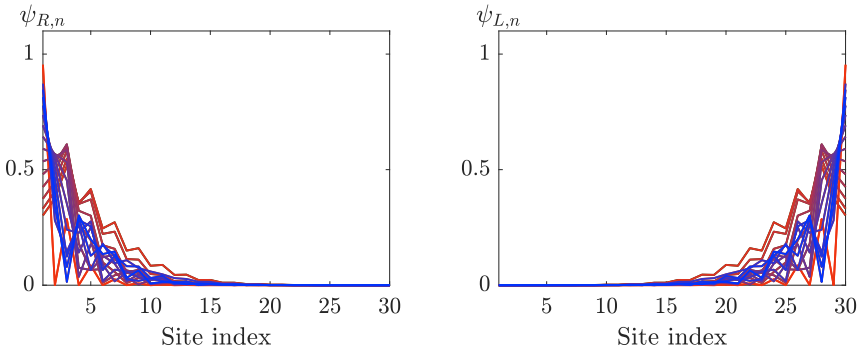

Figure 3.3: Exponentially localized right and left eigenvectors of the SSH-chain with parameter values $t_1 = 0.8$, $\gamma = 0.5$, $t_2 = 1$, and $N = 30$.

at in the periodic case. The skin effect, however, makes it less straightforward to interpret these states as bulk states, as we would have in the Hermitian case.

From the above discussion, it is clear that we cannot expect that a bulk invariant derived from the Bloch Hamiltonian should be related to the boundary states in the open system. Nevertheless, we could try to compute the winding number as we did for the Hermitian case in Sec. 2.1.3. However, we note that attempting to write the Bloch Hamiltonian in terms of the Pauli matrices, as we did in Eqs. (2.15)-(2.16), gives us

$$H_{\text{Bloch}}(k) = \mathbf{d}(k) \cdot \sigma, \tag{3.8}$$

with

$$d_x(k) = t_1 + t_2 \cos(k), \quad d_y(k) = t_2 \sin(k) - i\gamma, \quad d_z(k) = 0. \tag{3.9}$$

That is, $\mathbf{d}(k) \in \mathbb{C}^3$, which means that we can no longer even define the winding number in this way. (There are, however, attempts to define other types of invariants for the system, see e.g. [42, 93, 96].)

From all of the above, we thus see that essentially nothing remains of the bulk-boundary correspondence as we know it from the Hermitian case. In Ch. 4 we will see how we can formulate a new bulk-boundary correspondence, but before we come to that, we will study the sensitivity of the spectrum and eigenvectors in more detail.

3.3 Sensitivity to boundary conditions

In the previous section, we saw several phenomena that are related to the non-Hermiticity. It turns out that the sensitivity of the spectrum to boundary conditions, the skin effect and the type of gap in the system are related to each other.

In this section, we will formalize this and look into more detail on the effects and how they are related.

3.3.1 Non-Hermitian lattice models

As we saw in Sec. 2.1.2, the tight-binding matrix describing a lattice with rectangular geometry, will be a block-tridiagonal block-Toeplitz matrix. When we now attempt to generalize this to the non-Hermitian case, we notice that the block-structure will be intact. This means that we, for an n-dimensional system, get a Hamiltonian of the form

$$H_{nD} = \begin{pmatrix} H_{(n-1)D} & B_n & & \delta_n C_n \\ C_n & \ddots & \ddots & \\ & \ddots & \ddots & B_n \\ \delta_n B_n & & C_n & H_{(n-1)D} \end{pmatrix}, \tag{3.10}$$

where $H_{(n-1)D}$ is the not necessarily Hermitian matrix describing an $(n-1)$-dimensional system and B_n and C_n describe the couplings between these stacked systems. We also add a parameter $\delta_n \in [0, 1]$ which interpolates between open and periodic boundary conditions in the nth dimension. We introduce the subscript on the δ as we could imagine wanting to study different boundary conditions in different directions.

In Sec. 2.1.2 we made an analysis of the properties of the eigenvalues based on the interlacing theorem. This is no longer possible if our matrix is non-Hermitian, which should be clear in a situation where we e.g. have complex eigenvalues. Since not-necessarily-Hermitian matrices is a class containing all matrices, we cannot really expect there to be a perturbation theorem that gives us a very exact perturbation bound for all matrices. In general, there are some theorems that apply to all matrices. These theorems are not so restrictive, but still give a sense of an upper limit of how far away the eigenvalues can move given a specific perturbation. This, however, does not tell us a lot in reality since these limits still give room for significant qualitative change in spectra. And indeed, we see from examples that in some systems even a very small perturbation can lead to large changes in the spectrum, while in other systems this is not the case. We will now look closer at this. The ultimate goal would be to find conditions on the parameters in the lattice model that tell us whether or not the spectrum is sensitive to perturbations.

So far we have only spoken quite loosely about the sensitivity to boundary conditions, but as we see in the plots the change in spectrum appears to be quite drastic and it is of interest to understand this sensitivity more properly. In the

supplementary material of Paper I, we briefly study the SSH-chain with boundary conditions that interpolate between open and periodic boundary conditions. This is done by introducing a parameter $\delta \in [0, 1]$ in the following way,

$$H(\delta) = \begin{pmatrix} 0 & t_1+\gamma & & & & & \delta t_2 \\ t_1-\gamma & \ddots & t_2 & & & & \\ & t_2 & \ddots & t_1+\gamma & & & \\ & & t_1-\gamma & \ddots & \ddots & & \\ & & & \ddots & \ddots & t_1+\gamma & \\ \delta t_2 & & & & t_1-\gamma & 0 & \end{pmatrix}, \tag{3.11}$$

and studying what happens if δ is changed away from 0. It turns out that the larger the system is, the smaller the δ required for the spectrum to change away from the spectrum of the open system. More specifically it is observed that the δ required to change a point in the spectrum by a fixed amount ΔE seems to be proportional to $e^{-\alpha N}$, where N is the length of the chain.

That the sensitivity to boundary conditions seems to be exponential, has several implications, not least when doing numerical calculations. In Fig. 3.4, we show the eigenvalue spectrum for an SSH-model with open boundary conditions for several different system sizes. In these plots we have alternating hoppings $t_{r,1}$ and $t_{r,2}$ to the right and $t_{l,1}$ and $t_{l,2}$ to the left, respectively, with $t_{r,1} = 2$, $t_{r,2} = 4$, $t_{l,1} = 1$ and $t_{l,2} = 4$. It might seem as if the spectrum changes significantly with system size, but this is a numerical issue that probably has to do with the fact that the floating point representation of the numbers is not accurate enough and could also be affected by the algorithm used to compute the eigenvalues. This plot was made using MATLAB R2020b.

The fact that these systems are so prone to numerical errors, makes it very important to be aware of this when doing numerical calculations. It also makes it interesting to understand the sensitivity in more detail.

3.3.2 The spectral winding number and gaps

In previous section, we saw an example of the skin effect. In general we define the skin effect as the phenomenon that an extensive number of left and right eigenstates, in the system with open boundary conditions, are exponentially localized to one of the boundaries of the system. That this can occur in non-Hermitian systems is experimentally verified in several different contexts, see e.g. [30, 31, 35, 54, 97, 98].

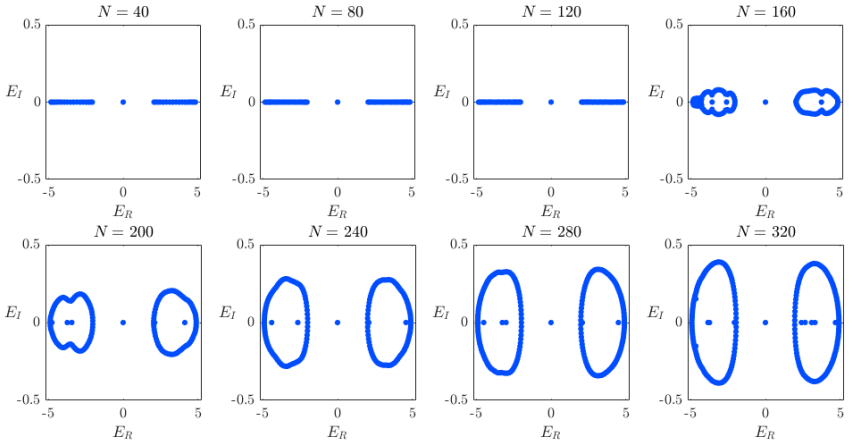

Figure 3.4: Eigenvalues of the SSH-chain with parameter values $t_{r,1} = 2$, $t_{r,2} = 4$, $t_{l,1} = 1$ and $t_{l,2} = 4$ numerically found using MATLAB R2020b for different system sizes. As N becomes larger, the system becomes numerically unstable and we see a deviation from the spectrum we expect for open boundary conditions into something that resembles the periodic case.

It is clear that if the boundary conditions are changed to periodic, something very drastic will happen in the system since there is no longer any boundary that the states can localize to, which means that the states will change from exponentially localized to completely delocalized. This suggests that there should also be a big change in the eigenvalue spectrum when there is a skin effect, just as we saw in the SSH-chain.

The skin effect is not present in all non-Hermitian systems, which in turn means that not all non-Hermitian systems need to have sensitive spectra. This can be seen in Fig. 3.5, where we, for an SSH-chain with parameter values $t_{r,1} = 0.5$, $t_{r,2} = 8$, $t_{l,1} = i$ and $t_{l,2} = 4$, plot the right eigenstates for the system with open boundary conditions together with the eigenvalues for both open and periodic boundary conditions. We see that, apart from the emergence of a zero mode in the case of open boundary conditions, the spectra are very similar and the eigenstates are delocalized. To predict when this happens in one-dimensional systems, and possibly find conditions on the parameter values in the system for when this occurs, one can use the spectral winding number defined in [46, 99] as

$$w(E_B) = \frac{1}{2\pi i} \int_{-\pi}^{\pi} \frac{d}{dk} \ln \det[H(k) - E_B] dk, \tag{3.12}$$

where $E_B \in \mathbb{C}$. We note that, while the winding number defined for the SSH-chain

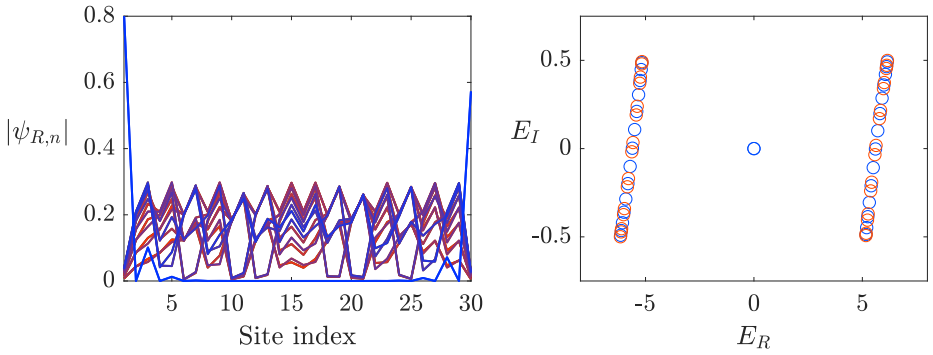

Figure 3.5: Left: Absolute value of right eigenvectors for an SSH-chain with parameter values $t_{r,1} = 0.5$, $t_{r,2} = 8$, $t_{l,1} = i$ and $t_{l,2} = 4$ and open boundary conditions. Right: Eigenvalues of the same SSH-chain for open (blue) and periodic (red) boundary conditions.

in Eq. (2.17) can be computed only since the vector $\mathbf{d}$ lies in a plane, the spectral winding number can be defined for any one-dimensional system.

If there exists an E_B for which $w(E_B)$ is non-zero, there will be a skin effect in the system, otherwise not. Since we have argued that the skin effect is tied to the sensitivity of the spectrum, this also implies that if we have a non-zero winding number for some E_B there will be a high sensitivity to boundary conditions. Closely related to this are the types of gaps that can be found in a non-Hermitian system [43, 46], namely, we differentiate between point gaps and line gaps, where the latter resembles the Hermitian case. A system with loops in the spectrum of the Bloch Hamiltonian is said to have a point gap, while a system where the spectrum of the Bloch Hamiltonian can be divided into two parts by a line is said to have a point gap. We note that since the determinant of a matrix is equal to the product of its eigenvalues, the spectral winding number can be rewritten as the sum of the windings of the eigenvalues of $H(k)$ around the point E_B [46], namely

$$w(E_B) = \sum_n \frac{1}{2\pi i} \int_{-\pi}^{\pi} \frac{E_n'(k)}{E_n(k) - E_B} dk, \tag{3.13}$$

where $E_n(k)$ is the nth eigenvalue of $H(k)$. This implies that a necessary, but not sufficient condition for having a skin effect is that there are loops in the spectrum of the Bloch Hamiltonian. Similarly, if we have a Bloch Hamiltonian whose spectrum does not have any point gaps, i.e. if it consists of line segments, the system cannot have a skin effect.

To give an example, we look at the Hatano-Nelson model, which is described by the Bloch Hamiltonian $H(k) = t_r e^{ik} + t_l e^{-ik}$. Just by looking at the form of $H(k)$,

we can see that the spectrum will form an ellipse if $|t_r| \neq |t_l|$ and a straight line segment otherwise. We can thus conclude that only if $|t_r| = |t_l|$, the winding of the spectrum will be zero around all points, and thus it is only at these parameter values we do not have a skin effect. We can try to do this using the integral instead:

$$w(E) = \frac{1}{2\pi i} \int_{-\pi}^{\pi} \frac{it_r e^{ik} - it_l e^{-ik}}{t_r e^{ik} + t_l e^{-ik} - E} dk. \tag{3.14}$$

This integral is relatively easy to compute, but it is enough to go to the SSH-model to realize that it quickly becomes very difficult to find the winding number analytically for arbitrary parameter values. A general one-band model has a Bloch Hamiltonian of the form

$$H(k) = t_0 + \sum_{n=1}^{m} (t_{-n} e^{-ikn} + t_n e^{ikn}), \tag{3.15}$$

where m describes the maximum hopping distance. It is clear that the winding number integral will become essentially impossible to evaluate analytically for arbitrary values of the t_ns for almost all such models, and thus we cannot expect that this integral will be a convenient way to find out for which combinations of parameter values the system might not have a skin effect.

We would therefore have to rely on other methods, like the one identifying the spectrum of the Hatano-Nelson model as an ellipse. Similar arguments can be made for other simple models, but again, in more complicated situations it will not be possible to fully determine analytically when we do and do not have a skin effect. This is, however, something that is important to try and understand further, which is what we do in Paper IV.

3.3.3 Quantifying the sensitivity

In Paper IV, we study matrices of the form in Eq. (3.10) and their sensitivity to boundary conditions. Apart from the sensitivity discussion in last section, this is important because, while the winding number predicts the presence of the skin effect in one-dimensional systems, it cannot be used in higher-dimensional systems. Therefore it is of interest to develop a complementary method to find the parameter values for which the system is insensitive.

One-dimensional systems

In the first part of Paper IV, we study one-dimensional systems with unit cells consisting of one site. These can be described by ordinary banded Toeplitz matrices, the hopping range determined by the number of non-zero diagonals in the

matrix. Using a parameter δ to interpolate between open and periodic boundary conditions, we thus want to find the eigenvalues of matrices of the form

$$H_{1D} = \begin{pmatrix} t_0 & t_1 & \dots & t_k & 0 & \dots & 0 & \delta t_{-k} & \dots & \delta t_{-1} \\ t_{-1} & t_0 & t_1 & & t_k & 0 & & \ddots & \ddots & \vdots \\ \vdots & t_{-1} & \ddots & \ddots & & \ddots & \ddots & & \ddots & \delta t_{-k} \\ t_{-k} & & \ddots & \ddots & \ddots & & \ddots & \ddots & & 0 \\ 0 & t_{-k} & & \ddots & \ddots & \ddots & & \ddots & 0 & \vdots \\ \vdots & 0 & \ddots & & \ddots & \ddots & \ddots & & t_k & 0 \\ 0 & & \ddots & \ddots & & \ddots & \ddots & \ddots & & t_k \\ \delta t_k & \ddots & & \ddots & \ddots & & \ddots & \ddots & t_1 & \vdots \\ \vdots & \ddots & \ddots & & 0 & t_{-k} & & t_{-1} & t_0 & t_1 \\ \delta t_1 & \dots & \delta t_k & 0 & \dots & 0 & t_{-k} & \dots & t_{-1} & t_0 \end{pmatrix}. \tag{3.16}$$

We do this by assuming a functional form in some parameter α of the eigenvalues that is determined from the solution to the $\delta = 1$ case. For such an eigenvalue $\lambda(\alpha)$, we now have a corresponding eigenvector v_α and the goal is to find the appropriate values of α since that gives us the eigenvalues. To do this, we go to the eigenvalue equation from which we get a recurrence relation for the elements of the vector v_α of the form

$$\sum_{n=1}^{k} (t_{-n} v_{\alpha,j-n} + t_n v_{\alpha,j+n}) + (t_0 - \lambda(\alpha)) v_j = 0. \tag{3.17}$$

The solution to this recurrence relation will contain a number of constants that can be determined using the boundary conditions, and in this process we also find the appropriate values of α. For details, see Paper IV.

For the simplest case, the Hatano-Nelson model, with $t_0 = t_d$, $t_1 = t_l$ and $t_{-1} = t_r$, we get that the eigenvalues are given by

$$\lambda = t_d + 2\sqrt{t_r}\sqrt{t_l}\cos(\tilde{\alpha}), \tag{3.18}$$

where the parameter $\tilde{\alpha}$ is given by the equation

$$\delta^2 \frac{\sin(\tilde{\alpha}(N-1))}{\sin(\tilde{\alpha})} + \delta\left(\frac{t_r^{N/2}}{t_l^{N/2}} + \frac{t_l^{N/2}}{t_r^{N/2}}\right) - \frac{\sin(\tilde{\alpha}(N+1))}{\sin(\tilde{\alpha})} = 0. \tag{3.19}$$

From this equation, we can see that the eigenvalues will be very sensitive to changes in δ when $|t_r| \neq |t_l|$, and that we can classify this sensitivity as exponential. On

the other hand, we see that the spectrum is relatively insensitive when $|t_r| = |t_l|$. This is in agreement with the computation of the winding number in Sec. 3.3.2. As we saw there, it is a very hard problem to compute the integral as an analytic function of the system parameters for more complicated systems. The method used in Paper IV, however, reaches further and we can get conditions on parameters for more complicated systems than what is possible using the winding number. This method also says more about the behavior of the eigenvalues as we explicitly see what happens when we change the boundary conditions. For example, we can see that the spectrum is very sensitive around $\delta = 0$, but relatively insensitive around $\delta = 1$. This explains the behavior in Fig. 3.4 – when the system size is increased, the numerical inaccuracies are enough to perturb the spectrum away from the open spectrum in such a way that it starts resembling the periodic one.

We can obtain more complicated one-dimensional systems by stacking one-dimensional chains with known eigenvalues in a periodic fashion. That is, we effectively get a two-dimensional system with periodic boundary conditions in one direction. This gives us clues about what relations between parameters in a system we can expect to give a system without a skin effect. We do this in Paper IV and see that a necessary condition for *not* having a skin effect seems to be that the system should be balanced in some way, meaning that the overall hopping to the left in the unit cell should be the same as the overall hopping to the right. A clear example of this is for the SSH-chain with alternating hoppings $t_{1,r}, t_{r,2}$ to the right and $t_{l,1}, t_{l,2}$ to the left, where the condition for not having a sensitive spectrum is

$$|t_{r,1}t_{r,2}| = |t_{l,1}t_{l,2}|. \tag{3.20}$$

This is quite intuitive as it would imply that there is no 'favored' edge in the system. However, this condition with an overall balancing does not seem to be sufficient in general as there are systems which seem to be balanced, but that still have a skin effect. One example of this is when we introduce longer range hoppings. In a system with only t_1 and t_{-2} non-zero, we see that there is no choice of t_1 and t_{-2} for which we do not have a skin effect – not even when they are equal.

Two-dimensional systems

As mentioned, the winding number can only be used for one-dimensional systems, and it would be desirable to find another way to predict the presence of the skin effect. This has been investigated in e.g. [100], but the results are somewhat inconclusive. Block-Toeplitz matrices describing systems with open boundary conditions are, however, notoriously hard to diagonalize analytically. Nevertheless, having obtained balancing conditions for two-dimensional systems with periodic boundary conditions in one direction, we can implement those conditions in two dimensions

and hope to find systems without skin effect that are purely two-dimensional. This works, and we show e.g. that the triangular lattice can be obtained in this way as a lattice with no skin effect. At least when the number of unit cells in both directions are the same. When they are different, we notice that the states start to localize even though the parameters indicate the system should be balanced. This is contrary to the intuitive explanation given in Paper II for the absence of the skin effect in the triangular kagome lattice, where we argued that this could be due to the formation of closed loops that prevent the states from getting 'trapped' at a corner, but this is clearly not the whole story, despite its intuitiveness.

Chapter 4

Biorthogonal quantum mechanics

In order to understand the strange effects we saw in Sec. 3.2 and formulate a new kind of bulk-boundary correspondence, we will turn to the formalism of biorthogonal quantum mechanics, which is described in [68, 101]. It was originally developed as an extension of Hermitian quantum physics to allow for Hamiltonians that are non-Hermitian, but still have real eigenvalues, as is the case for PT-symmetric systems, but we will apply it in a more general setting. In this section, we will first describe some general theory, and then show how one can apply it in the context of lattice systems.

4.1 The biorthogonal inner product

We start by giving an introduction to the biorthogonal formalism described in [68]. Suppose we have an operator H, which is not necessarily Hermitian, on a *finite-dimensional* Hilbert space. (The infinite-dimensional case is complicated, and something one needs to be very careful with.) We will typically think of H as a Hamiltonian. Denote the right eigenstates of this operator by $|R_n\rangle$ and the left eigenstates by $\langle L_n|$, and let them correspond to the eigenvalue E_n. That is, let

$$H\,|R_n\rangle = E_n\,|R_n\rangle\,, \quad \langle L_n|\,H = E_n\,\langle L_n|\,. \tag{4.1}$$

One of the most important properties of the eigenstates of the Hamiltonian in Hermitian quantum mechanics is the fact that they can always be chosen to be orthogonal to each other. This implies that the eigenstates of the Hamiltonian are stationary states and also greatly simplifies computations of e.g. probabilities. If the Hamiltonian is non-Hermitian, this is no longer necessarily true. This means

that if we were to do quantum mechanics the way we are used to, we 1) would get a lot of complicated calculations and 2) might miss out on information about the system since the left eigenstates may contain information that the right ones do not. Furthermore, it actually leads to contradictions. The probability in quantum mechanics to transition from a normalized state $|\alpha\rangle$ into another normalized state $|\beta\rangle$ is given by $|\langle\beta|\alpha\rangle|^2$. We now see that if we have a non-Hermitian Hamiltonian, the probability to transition from one eigenstate $|R_n\rangle$ into another state $|R_m\rangle$ is given by $|\langle R_m|R_n\rangle|^2$, which is not necessarily zero since the eigenstates might not be orthogonal. This contradicts the fact that we want the eigenstates to be stationary with zero transition probability between them.

The solution to this is to define a new inner product that we use to do computations of e.g. probabilities. We note that instead of orthogonality between right eigenstates, we have

$$\langle L_n|R_m\rangle = \delta_{mn}, \tag{4.2}$$

which in the Hermitian case reduces to the ordinary orthogonality among the eigenstates.

Since the sets of left and right eigenstates form two linearly independent sets respectively, we can expand an arbitrary state $|\alpha\rangle$ in the right eigenstates:

$$|\alpha\rangle = \sum_n a_n |R_n\rangle . \tag{4.3}$$

Now we define the state $|\tilde{\alpha}\rangle$ as

$$|\tilde{\alpha}\rangle = \sum_n a_n |L_n\rangle . \tag{4.4}$$

Normally, in quantum mechanics, we have a Hilbert space $\mathscr{H}$ consisting of states $|\alpha\rangle$. To each of these states, we associate in a unique way a state $\langle\alpha|$ in the dual Hilbert space $\mathscr{H}^*$. Now, instead of associating the state $\langle\alpha|$ to $|\alpha\rangle$, we pick the state $\langle\tilde{\alpha}| \in \mathscr{H}^*$, and we thus call $|\tilde{\alpha}\rangle$ the *associated state* of $|\alpha\rangle$. Clearly, as long as the space is finite dimensional and the Hamiltonian is diagonalizable, this association is unique and well-defined. Using this, we define the *biorthogonal inner product* of the states $|\alpha\rangle$ and $|\beta\rangle = \sum_n b_n |R_n\rangle$ as

$$(|\alpha\rangle , |\beta\rangle) = \langle\tilde{\alpha}|\beta\rangle = \sum_n a_n^* b_n. \tag{4.5}$$

That this is an inner product can easily be seen by first noting that it clearly is linear in its second argument and anti-linear in the first. Furthermore, we have

$$\langle\tilde{\beta}|\alpha\rangle^* = \sum_n b_n a_n^* = \langle\tilde{\alpha}|\beta\rangle , \tag{4.6}$$

and finally,

$$(|\alpha\rangle, |\alpha\rangle) = \langle\tilde{\alpha}|\alpha\rangle = \sum_n a_n^* a_n = \sum_n |a_n|^2 \geqslant 0. \tag{4.7}$$

The final equality in Eq. (4.5) shows that the inner product in this case works in the way we are used to in Hermitian quantum mechanics. However, some care is needed as this equality is not necessarily true if we make a change of basis, meaning that the coefficients in another basis might not correspond to probability amplitudes. From now on we will normalize all states according to this inner product. That is, we normalize a state $|\Psi\rangle$ by requiring $\langle\tilde{\Psi}|\Psi\rangle = 1$.

Assuming that all the states $|R_n\rangle$, $|L_n\rangle$ and $|\alpha\rangle$ are normalized, we get for the state $|\alpha\rangle$ that

$$(|\alpha\rangle, |\alpha\rangle) = \sum_n a_n^* a_n = 1, \tag{4.8}$$

and we can interpret the number $a_n^* a_n = \langle L_n|\alpha\rangle \langle\tilde{\alpha}|R_n\rangle$ as the probability to transition from the state $|\alpha\rangle$ into the nth eigenstate of the Hamiltonian. In particular, we see that if $|\alpha\rangle$ is an eigenstate of H, then the probability is, just as we expect, 1 to remain in that state and 0 to transition into another state.

More generally, we now get that the probability to transition from a state $|\alpha\rangle$ into another state $|\beta\rangle$ is given by

$$P = \frac{\langle\tilde{\alpha}|\beta\rangle \langle\tilde{\beta}|\alpha\rangle}{\langle\tilde{\alpha}|\alpha\rangle \langle\tilde{\beta}|\beta\rangle}. \tag{4.9}$$

This is a real number, and because of the Cauchy-Schwartz inequality, it must also be a number between 0 and 1, which means that it can be interpreted as a probability. That it makes sense to define probabilities in this way is further discussed in [68].

Using the fact that we can talk about probabilities, we can also find an expression for the expectation value of an operator A. Namely, we define the expectation value of the operator A in the normalized state $|\alpha\rangle$ as

$$\langle A\rangle = \frac{(|\alpha\rangle, A|\alpha\rangle)}{(|\alpha\rangle, |\alpha\rangle)} = \frac{\langle\tilde{\alpha}|A|\alpha\rangle}{\langle\tilde{\alpha}|\alpha\rangle}. \tag{4.10}$$

If A happens to be the Hamiltonian, we get

$$\langle H\rangle = \frac{\langle\tilde{\alpha}|H|\alpha\rangle}{\langle\tilde{\alpha}|\alpha\rangle} = \frac{\sum_n a_n^* a_n E_n}{\sum_n a_n^* a_n}, \tag{4.11}$$

which we see is precisely the expression that we expect.

We note that the expectation value does not always have to be real since non-Hermitian operators can have complex valued eigenvalues. However, if the Hamiltonian has real eigenvalues, also the expectation value of it is real. In general, an operator is said to be *biorthogonally Hermitian* if the matrix representation of it in the biorthogonal basis is a Hermitian matrix. This implies that the eigenvalues are real, and thus observables are naturally described by biorthgonally Hermitian operators, rather than Hermitian operators, in biorthogonal quantum mechanics.

In summary, we see that given a Hamiltonian H and a set of left and right eigenstates, we can define an inner product that gives us a Hilbert space where physical states are represented as vectors and observables as biorthogonally Hermitian operators.

4.2 The bulk-boundary correspondence

Now we turn to applying the biorthogonal formalism described in [68] to some systems. The goal is to describe non-Hermitian versions of the systems that we introduced in Ch. 2. It is important to note here that we allow for non-Hermitian Hamiltonians with complex eigenvalues, which means that they can be used to describe interactions with the environment. This is different from what is done in [68] where the Hamiltonian is assumed to have real eigenvalues and describe a closed quantum system.

4.2.1 Lattices

Suppose we have a lattice with M sites. For notational simplicity we assume no internal degrees of freedom. The Hilbert space is then M-dimensional and the Hamiltonian will generically have M left and right eigenstates respectively. These are the states we use to define the inner product. Now, just as we are used to, another basis for the Hilbert space in this case is formed by the vectors represented by the standard basis vectors, that is the vectors containing precisely one element equal to 1 while the rest of the elements are zero. We will denote these vectors by $|e_k\rangle$ where k denotes a site in the lattice.

Just as in the Hermitian case, we can now consider the projection operator that projects a state onto the kth site. We take this operator to mean the operator that picks out the coefficient in front of $|e_k\rangle$ when writing the state as a linear combination of these vectors. This operator is given by

$$\Pi_k = |e_k\rangle \langle e_k| . \tag{4.12}$$

One might be skeptical about this, since in the biorthogonal formalism, it might

be more natural to take the projection operator to be $|e_k\rangle\langle\tilde{e}_k|$. But as we will see, the operator in Eq. (4.12) has nice properties that we want to take advantage of.

By considering the biorthogonal expectation value of Π_k in some state, we can get a measure of the localization of the state in the system, just as in the Hermitian case. Suppose we are interested in the mth eigenstate of the Hamiltonian. The biorthogonal expectation value of Π_k in this state is then given by

$$\langle\Pi_k\rangle = \langle L_m|\Pi_k|R_m\rangle = \langle L_m|e_k\rangle\langle e_k|R_m\rangle \tag{4.13}$$

Now, suppose

$$|R_m\rangle = \sum_n c_n^{(Rm)}|e_n\rangle\,, \quad |L_m\rangle = \sum_n c_n^{(Lm)}|e_n\rangle\,. \tag{4.14}$$

Inserting this into Eq. (4.13), we get

$$\langle\Pi_k\rangle = (c_k^{Lm})^* c_k^{Rm}. \tag{4.15}$$

Contrary to the Hermitian case, this number does not have to be real since the left and right eigenstates typically are different in non-Hermitian systems. We can, however, still use the result to get a sense of the localization of the state, by considering e.g. the absolute value of the expectation value. By collecting all these absolute values into a vector

$$\mathbf{\Pi}_\alpha = \sum_n \left|\frac{\langle\tilde{\alpha}|\Pi_n|\alpha\rangle}{\langle\tilde{\alpha}|\alpha\rangle}\right| |e_n\rangle \doteq \begin{pmatrix} |\langle\Pi_1\rangle| \\ \vdots \\ |\langle\Pi_N\rangle| \end{pmatrix}, \tag{4.16}$$

we get a vector that can give us a sense of the localization of the state $|\alpha\rangle$ in the lattice.

4.2.2 The biorthogonal bulk-boundary correspondence

Now, let us apply the above to the non-Hermitian systems of interest. For simplicity, we do this again in the SSH-chain described in Sec. 3.2, as was done in Paper I. In Fig. 4.1 we plot the absolute value of the biorthogonal expectation value of Π_n as a function of n for the eigenstates of a system with parameter values $t_1 = 0.8$, $\gamma = 0.5$, $t_2 = 1$, and $N = 30$. For these parameter values, we expect a skin effect as we can see in Fig. 3.3, but remarkably we see no such thing in Fig. 4.1. Instead we see a behavior that resembles what we are used to from the Hermitian case in terms of bulk and boundary states. Namely, we notice that the vector $\mathbf{\Pi}$ is delocalized for almost all states. The states for which this is the case, we call

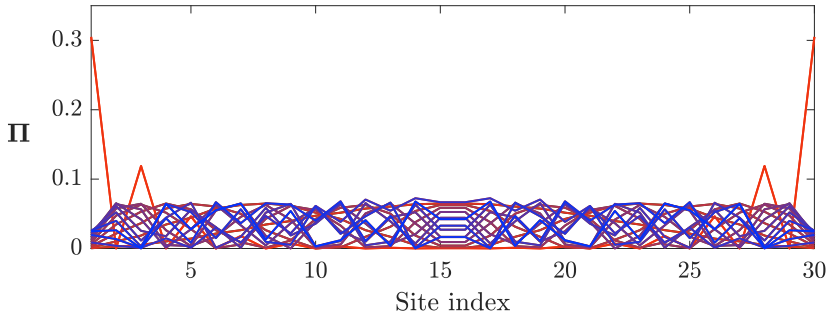

Figure 4.1: The vector **Π** for each of the eigenstate in an SSH-chain with parameter values $t_1 = 0.8$, $\gamma = 0.5$, $t_2 = 1$, and $N = 30$. These are the same parameter values as in Fig. 3.3 where we see a clear skin effect.

biorthogonal bulk states. In a similar fashion, we see that we have two states for which **Π** is localized to the ends of the chain, and we thus call these *biorthogonal boundary state*. It therefore seems like we can use the biorthogonal expectation value of Π_k to define bulk and boundary states in non-Hermitian systems.

Now the question is if we can use gap closings etc. to predict the existence of biorthogonal boundary states. To investigate this, we use the same method as was used in Sec. 2.2.1 for Hermitian systems; we begin by studying the system with an odd number of sites, i.e. with a broken unit cell. For this system, we have for all parameter values a zero eigenvalue with corresponding left and right eigenstates

$$\begin{aligned} |\psi_R\rangle &= \mathcal{N}_R \sum_n r_R^n c_{n,A}^\dagger |0\rangle , \\ |\psi_L\rangle &= \mathcal{N}_L \sum_n r_L^n c_{n,A}^\dagger |0\rangle , \end{aligned} \tag{4.17}$$

where $r_R = -(t_1 - \gamma)/t_2$ and $r_L^* = -(t_1 + \gamma)/t_2$.

Computing the biorthogonal expectation value of Π_n in this state, we get

$$\langle \Pi_n \rangle = \langle \psi_L | \Pi_n | \psi_R \rangle = \mathcal{N}_R \mathcal{N}_L^* (r_L^* r_R)^n, \tag{4.18}$$

and we see that just as in the Hermitian case, the vector **Π** will be localized to different sides of the chain for different parameter values. In this case, it is delocalized when

$$|r_L^* r_R| = 1, \tag{4.19}$$

which happens when

$$\left| \frac{t_1^2 - \gamma^2}{t_2^2} \right| = 1. \tag{4.20}$$

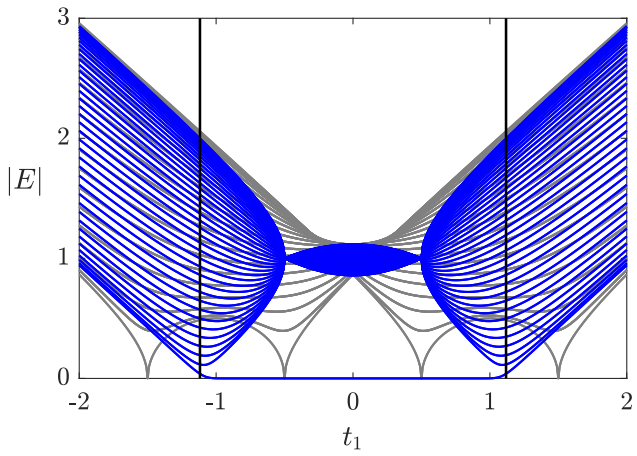

Figure 4.2: Absolute value of the energy spectra of the non-Hermitian SSH model for $t_2 = 1$, $\gamma = 0.5$, and $N = 40$ unit cells and different boundary conditions. Blue lines correspond to open boundary conditions and gray lines to periodic boundary conditions. The black lines correspond to points predicted in Eq. (4.21) and we see that this corresponds to the gap closings in the spectrum with open boundary conditions.

Assuming that the parameters are real, this gives us the points

$$t_1 = \pm\sqrt{\gamma^2 - t_2^2}, \quad \text{and} \quad t_1 = \pm\sqrt{\gamma^2 + t_2^2}. \tag{4.21}$$

Furthermore, we note that for $|r_L^* r_R| > 1$, the state will be localized to the right of the chain and for $|r_L^* r_R| < 1$ to the left. This means, that in the chain with an even number of sites, i.e. with an unbroken unit cell, we should have biorthogonal boundary states for $|r_L^* r_R| < 1$. Comparing with the spectrum in Fig. 4.2, we see that this corresponds precisely to when we have a zero eigenvalue in the system. It thus seems the biorthogonal formalism is suitable for understanding these systems. Further confirmation of this is given by the biorthogonal polarization, also defined in Paper I,

$$P = 1 - \lim_{N\to\infty} \frac{1}{N} \sum_n n \frac{\langle \psi_L | \Pi_n | \psi_R \rangle}{\langle \psi_L | \psi_R \rangle}. \tag{4.22}$$

It turns out that we have $P = 1$ when we have a biorthogonal boundary state and $P = 0$, when we do not.

Similar effects can be seen in other systems and in Paper I we look at a two-dimensional Rice-Mele model [102] with non-Hermitian hoppings. In Paper II, we study systems of higher dimension. In particular, we study non-Hermitian versions of the systems described in Sec. 2.2.2 and 2.2.3. Using the biorthogonal formalism,

we find that there can exist both biorthogonal boundary and corner states, that become non-Hermitian analogues of higher-order states.

Further exploring of the use of the biorthogonal inner product is done in Paper III, where we define a generalized biorthogonal polarization. For a one-dimensional system with M boundary states we have

$$P = M - \lim_{N\to\infty} \frac{1}{N} \sum_{m=1}^{M} \sum_{n=1}^{N} n \frac{\langle \psi_{m,L} | \Pi_n | \psi_{m,R} \rangle}{\langle \psi_{m,L} | \psi_{m,R} \rangle}, \tag{4.23}$$

where m labels the boundary state. We show that P is equal to the number of biorthogonal boundary states in the system and thus we once again get a confirmation that the biorthogonal formalism is what we need to use to understand the gap closings.

The relationship between the gap closings in the spectrum of the systems with open boundary conditions and the appearance of biorthogonal boundary states is called the *biorthogonal bulk-boundary correspondence*. This has not only been studied theoretically, but has been verified experimentally in e.g. mechanical systems [35], where the mechanical system in question can be mapped to a non-Hermitian SSH-chain. They show that the right eigenstates can be directly probed and that the gap closings occur at the theoretically predicted points in Eq. (4.21). In [103] it is further argued that not only should one be able to probe the right eigenstates, but also should be able to probe the left eigenstates and thus find the full biorthogonal nature of the system.

4.3 The bulk states

In paper III, apart from studying boundary states in one-dimensional systems, we also generalize the method for finding bulk states described in Sec. 2.3, and we find all the bulk states of a non-Hermitian SSH-chain. In the system with a broken unit cell, we find they are of the form

$$\Psi_{R,\mathrm{Bulk},\pm}(k) = \mathcal{N}_R \begin{pmatrix} \Psi_{R,\mathrm{Bulk},\pm,A}(k,1) \\ \Psi_{R,\mathrm{Bulk},\pm,B}(k,1) \\ \Psi_{R,\mathrm{Bulk},\pm,A}(k,2) \\ \Psi_{R,\mathrm{Bulk},\pm,B}(k,2) \\ \vdots \\ \Psi_{R,\mathrm{Bulk},\pm,B}(k,N-1) \\ \Psi_{R,\mathrm{Bulk},\pm,A}(k,N) \end{pmatrix}, \tag{4.24}$$

where $\mathcal{N}_R$ is a normalization factor,

$$\Psi_{R,\text{Bulk},\pm,A}(k,n) = 2i\frac{(t_1-\gamma)^{n/2}}{(t_1+\gamma)^{n/2}}\left[(t_1+\gamma)\sin(kn) + t_2\frac{\sqrt{t_1+\gamma}}{\sqrt{t_1-\gamma}}\sin(k[n-1])\right], \tag{4.25}$$

and

$$\Psi_{R,\text{Bulk},\pm,B}(k,n) = 2i\frac{(t_1-\gamma)^{n/2}}{(t_1+\gamma)^{n/2}}E_\pm(k)\sin(kn). \tag{4.26}$$

The parameter k takes values $k = \pi j/N$ for $j = 1,\ldots,N-1$ and the number $E_\pm(k)$ is given by

$$E_\pm(k) = \pm\sqrt{t_1^2+t_2^2-\gamma^2+2t_2\sqrt{t_1-\gamma}\sqrt{t_1+\gamma}\cos(k)}, \tag{4.27}$$

and is the eigenvalue of the state $\Psi_{R,\text{Bulk},\pm}(k)$.

We notice that there are $2N-2$ such states, which means we have found all of them, since there also is an edge state given by Eq. (4.17). We notice that all these states show a clear exponential localization (not in the biorthogonal sense, but in the 'standard', Hermitian sense) to the side of the chain, as is expected from the skin effect. A similar phenomenon is also observed in Paper IV, where we study a more general SSH-chain and find the behavior of the bulk states.

From the right eigenstates we can, using the symmetry of the Hamiltonian, which implies that $\Psi_{L,\text{Bulk},\pm}(k,\gamma) \propto \Psi^*_{R,\text{Bulk},\pm}(k,-\gamma)$, conclude that the corresponding left eigenstates have the form

$$\Psi_{L,\text{Bulk},\pm}(k) = \mathcal{N}_L^*\begin{pmatrix}\Psi^*_{L,\text{Bulk},\pm,A}(k,1)\\ \Psi^*_{L,\text{Bulk},\pm,B}(k,1)\\ \Psi^*_{L,\text{Bulk},\pm,A}(k,2)\\ \Psi^*_{L,\text{Bulk},\pm,B}(k,2)\\ \vdots\\ \Psi^*_{L,\text{Bulk},\pm,B}(k,N-1)\\ \Psi^*_{L,\text{Bulk},\pm,A}(k,N)\end{pmatrix}, \tag{4.28}$$

where $\mathcal{N}_L$ is a normalization factor such that $\Psi_{L,\text{Bulk},\pm}(k)^*\Psi_{R,\text{Bulk},\pm}(k) = 1$,

$$\Psi_{L,\text{Bulk},\pm,A}(k,n) = 2i\frac{(t_1+\gamma)^{n/2}}{(t_1-\gamma)^{n/2}}\left[(t_1-\gamma)\sin(kn) + t_2\frac{\sqrt{t_1-\gamma}}{\sqrt{t_1+\gamma}}\sin(k[n-1])\right], \tag{4.29}$$

and

$$\Psi_{L,\text{Bulk},\pm,B}(k,n) = 2i\frac{(t_1+\gamma)^{n/2}}{(t_1-\gamma)^{n/2}}E_\pm(k)\sin(kn). \tag{4.30}$$

We would like to use these bulk states to study what happens as we approach the exceptional points at $t_1 = \pm\gamma$, but as they are written now, it seems like we end up with singularities. This is, however, only a matter of scaling; since they are eigenstates, we can multiply them by an appropriate factor and still have eigenstates. We thus pick the normalization factors $\mathcal{N}_R$ and $\mathcal{N}_L$ such that we have

$$\begin{aligned}
\Psi_{R,\text{Bulk},\pm,A}(k,n) =&(t_1-\gamma)^{(n-1)/2}(t_1+\gamma)^{(N-n-1)/2}\times \\
&\left[(t_1+\gamma)\sin(kn) + t_2\frac{\sqrt{t_1+\gamma}}{\sqrt{t_1-\gamma}}\sin(k[n-1])\right], \\
\Psi_{R,\text{Bulk},\pm,B}(k,n) =&(t_1-\gamma)^{(n-1)/2}(t_1+\gamma)^{(N-n-1)/2}E_\pm(k)\sin(kn), \\
\Psi_{L,\text{Bulk},\pm,A}(k,n) =&(t_1+\gamma)^{(n-1)/2}(t_1-\gamma)^{(N-n-1)/2}\times \\
&\left[(t_1-\gamma)\sin(kn) + t_2\frac{\sqrt{t_1-\gamma}}{\sqrt{t_1+\gamma}}\sin(k[n-1])\right], \\
\Psi_{L,\text{Bulk},\pm,B}(k,n) =&(t_1+\gamma)^{(n-1)/2}(t_1-\gamma)^{(N-n-1)/2}E_\pm(k)\sin(kn).
\end{aligned} \tag{4.31}$$

We see that in this case, we have no singularities as we approach the exceptional points. In addition, they are also not all equal to zero, so the limits are well-defined. We have

$$\lim_{t_1\to\gamma}\Psi_{R,\text{Bulk},\pm}(k) = (2\gamma)^{N/2}\sin(k)\begin{pmatrix}1\\ t_2/(2\gamma)\\ t_2/(2\gamma)\\ 0\\ \vdots\\ 0\end{pmatrix}, \tag{4.32}$$

and

$$\lim_{t_1\to\gamma}\Psi_{L,\text{Bulk},\pm}(k) = (2\gamma)^{N/2}\sin(k(N-1))\begin{pmatrix}0\\ \vdots\\ 0\\ t_2/(2\gamma)\\ t_2/(2\gamma)\end{pmatrix}, \tag{4.33}$$

and

$$\lim_{t_1\to-\gamma}\Psi_{R,\text{Bulk},\pm}(k) = (-2\gamma)^{N/2}\sin(k(N-1))\begin{pmatrix}0\\ \vdots\\ 0\\ -t_2/(2\gamma)\\ -t_2/(2\gamma)\end{pmatrix}, \tag{4.34}$$

and

$$\lim_{t_1\to-\gamma}\Psi_{L,\mathrm{Bulk},\pm}(k)=(-2\gamma)^{N/2}\sin(k)\begin{pmatrix}1\\-t_2/(2\gamma)\\-t_2/(2\gamma)\\0\\\vdots\\0\end{pmatrix}. \tag{4.35}$$

We notice that these states at the exceptional points cannot be normalized according to Eq. (4.2). However, away from the exceptional points, we can attempt to make such a normalization. We have

$$\begin{aligned}\Psi^{\dagger}_{L,\mathrm{Bulk},\pm}(k)\Psi_{R,\mathrm{Bulk},\pm}(k)&=\sum_{n=1}^{N}\Psi_{L,\mathrm{Bulk},\pm,A}(k,n)\Psi_{R,\mathrm{Bulk},\pm,A}(k,n)\\&+\sum_{n=1}^{N-1}\Psi_{L,\mathrm{Bulk},\pm,B}(k,n)\Psi_{R,\mathrm{Bulk},\pm,B}(k,n)\\&=N(t_1-\gamma)^{N/2-1}(t_1+\gamma)^{N/2-1}E_{\pm}(k)^2.\end{aligned} \tag{4.36}$$

We clearly see that this is 0 at the exceptional points, so we cannot normalize the states there, but away from the exceptional points, we get

$$\begin{aligned}\Psi_{R,\mathrm{Bulk},\pm,A}(k,n)=&\frac{1}{\sqrt{N}E_{\pm}(k)}\frac{(t_1+\gamma)^{(N-2n)/4}}{(t_1-\gamma)^{(N-2n)/4}}\times\\&\left[(t_1+\gamma)\sin(kn)+t_2\frac{\sqrt{t_1+\gamma}}{\sqrt{t_1-\gamma}}\sin(k[n-1])\right],\\\Psi_{R,\mathrm{Bulk},\pm,B}(k,n)=&\frac{1}{\sqrt{N}}\frac{(t_1+\gamma)^{(N-2n)/4}}{(t_1-\gamma)^{(N-2n)/4}}\sin(kn),\\\Psi_{L,\mathrm{Bulk},\pm,A}(k,n)=&\frac{1}{\sqrt{N}E_{\pm}(k)}\frac{(t_1-\gamma)^{(N-2n)/4}}{(t_1+\gamma)^{(N-2n)/4}}\times\\&\left[(t_1-\gamma)\sin(kn)+t_2\frac{\sqrt{t_1-\gamma}}{\sqrt{t_1+\gamma}}\sin(k[n-1])\right],\\\Psi_{L,\mathrm{Bulk},\pm,B}(k,n)=&\frac{1}{\sqrt{N}}\frac{(t_1-\gamma)^{(N-2n)/4}}{(t_1+\gamma)^{(N-2n)/4}}\sin(kn).\end{aligned} \tag{4.37}$$

We can clearly see that the limit as we approach the exceptional points is no longer well-defined. We thus have to make a choice between having an appropriate limit at the exceptional points and the states being normalized away from them. Even though perhaps inconvenient, it is not very surprising. The biorthogonal formalism

requires a complete set of eigenstates, and thus we cannot expect it to work at points where this is no longer true.

Eq. (4.37) shows us that the left and right eigenstates are symmetric, which is nice, but in principle there is nothing that prevents us from letting $\mathcal{N}_R$ and $\mathcal{N}_L$ being different, as long as we keep

$$\Psi^\dagger_{L,\text{Bulk},\pm}(k)\Psi_{R,\text{Bulk},\pm}(k) = 1. \tag{4.38}$$

As we will see in the next section, this can have consequences for the results.

4.4 Degree of freedom in the biorthogonal inner product

Applying the definition of the biorthogonal inner product to our systems, gives us a degree of freedom, namely, the eigenvectors of an operator are only determined up to a scale factor. This means that any set of right eigenvectors of a Hamiltonian together with an appropriately normalized set of left eigenvectors form a valid biorthogonal basis that can be used to define the biorthogonal inner product. This poses a possible problem, as is pointed out in e.g. [104, 105] and something we investigate further in Paper V.

Suppose we have a Hamiltonian H with a set of left and right eigenstates $\{|L_n\rangle\}$ and $\{|R_n\rangle\}$ such that $\langle L_n|R_n\rangle = 1$. Suppose further that there exists another set of eigenstates $\{|L'_n\rangle = \alpha_n |L_n\rangle\}$ and $\{|R'_n\rangle = \alpha_n^{-1} |R_n\rangle\}$. Both of these sets can be used to define a biorthogonal inner product according to Eq. (4.5). Let us denote these inner products by $(-,-)$ and $(-,-)'$ respectively. Now, suppose we have a vector

$$|\alpha\rangle = \sum_n a_n |R_n\rangle = \sum_n \frac{a_n}{\alpha_n} |R'_n\rangle . \tag{4.39}$$

The associated states in the respective biorthogonal bases now become

$$|\tilde{\alpha}\rangle = \sum_n a_n |L_n\rangle , \tag{4.40}$$

and

$$|\tilde{\alpha}'\rangle = \sum_n \frac{a_n}{\alpha_n} |L'_n\rangle . \tag{4.41}$$

Computing the probability of measuring energy E_n for a particle in a state represented by the vector $|\alpha\rangle$ in the respective inner products gives us

$$p_n = \frac{(|\alpha\rangle , |R_n\rangle)(|R_n\rangle , |\alpha\rangle)}{(|\alpha\rangle , |\alpha\rangle)(|R_n\rangle , |R_n\rangle)} = \frac{\langle L_n|\alpha\rangle \langle\tilde{\alpha}|R_n\rangle}{\langle\tilde{\alpha}|\alpha\rangle \langle L_n|R_n\rangle} = \frac{c_n^* c_n}{\sum_m c_m^* c_m}, \tag{4.42}$$

and

$$p'_n = \frac{(|\alpha\rangle, |R_n\rangle)'(|R_n\rangle, |\alpha\rangle)'}{(|\alpha\rangle, |\alpha\rangle)'(|R_n\rangle, |R_n\rangle)'} = \frac{\langle L'_n|\alpha\rangle \langle\tilde{\alpha}'|R'_n\rangle}{\langle\tilde{\alpha}'|\alpha\rangle \langle L'_n|R'_n\rangle} = \frac{\frac{c_n^* c_n}{\alpha_n^* \alpha_n}}{\sum_m \frac{c_m^* c_m}{\alpha_m^* \alpha_m}}. \tag{4.43}$$

Clearly, the probability here depends on the choice of α_n. In a similar fashion, we expect the expectation value to depend on that choice as well. To illustrate this, we compute the biorthogonal expectation value of an operator Q in the state represented by the vector $|\alpha\rangle$ using the different inner products:

$$\langle Q\rangle = \frac{\langle\tilde{\alpha}|Q|\alpha\rangle}{\langle\tilde{\alpha}|\alpha\rangle} = \frac{\sum_{mn} a_m^* a_n \langle L_m|Q|R_n\rangle}{\sum_n a_n^* a_n}, \tag{4.44}$$

and

$$\langle Q\rangle' = \frac{\langle\tilde{\alpha}'|Q|\alpha\rangle}{\langle\tilde{\alpha}'|\alpha\rangle} = \frac{\sum_{mn} \frac{a_m^* a_n}{\alpha_m^* \alpha_n} \langle L_m|Q|R_n\rangle}{\sum_n \frac{a_n^* a_n}{\alpha_n^* \alpha_n}}, \tag{4.45}$$

These are clearly not equal in general, which means that the expectation value depends on which biorthogonal basis we pick. This in itself is not necessarily a problem, since we change the Hilbert space when we change the inner product, and thus we also change the way our states and operators are represented. Thus the vector $|\alpha\rangle$ can describe different physical states depending on which inner product we use. However, when we study the non-Hermitian lattice models, we take the vectors $|e_n\rangle$ to represent positions in the lattice, which means that we assign a meaning to the vector itself, irrespective of which inner product is used. To illustrate the consequences of this, we consider as an example the Hatano-Nelson model with

$$H(\gamma) = \begin{pmatrix} 0 & t+\gamma & & \\ t-\gamma & \ddots & \ddots & \\ & \ddots & \ddots & t+\gamma \\ & & t-\gamma & 0 \end{pmatrix} \tag{4.46}$$

Now, suppose we want to find the expectation value of H in the state $|e_1\rangle + |e_2\rangle$. We do this using two different choices of eigenvectors of the Hamiltonian, while still keeping the Brody normalization. The choices are the following:

IP1. We pick $\langle R_n|R_n\rangle = \langle L_n|L_n\rangle$ and $\langle L_n|R_n\rangle = 1$.

IP2. We pick $\langle R_n|R_n\rangle$ randomly and then choose $|L_n\rangle$ according to $\langle L_n|R_n\rangle = 1$.

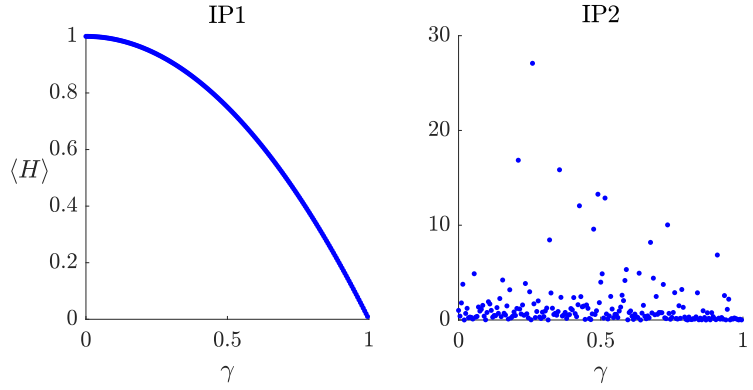

Figure 4.3: The expectation value of the Hamiltonian in the state $|e_1\rangle + |e_2\rangle$ as a function of γ using two different choices of normalization of the eigenstates of the Hamiltonian.

We depict the differences between these choices as a function of γ in Fig. 4.3, where we can see that the expectation value as a function of γ shows a significant qualitative change when we change the definition of the inner product. This obviously raises some questions and makes it very important to make sure that the results obtained in Papers I-III are consistent.

The most important observation we make in this context is that if $|\alpha\rangle$ is an eigenstate of H, then Eqs. (4.44) and (4.45) are independent of the choice of eigenvectors of the Hamiltonian, and thus all expectation values will be the same irrespective of normalization of the eigenstates of the Hamiltonian. The biorthogonal bulk-boundary correspondence described in Papers I-III is a statement about properties of eigenstates of the Hamiltonian, and thus all the results in these papers will be unaffected by the ambiguity.

However, the issue remains if one would want to study such families of lattice models further. For example, a natural question could be what would happen to a particle that is placed on the nth site in the lattice, but since the meaning of the vector $|e_n\rangle$ is ambiguous, it is not clear how to tackle this given the above. All in all there are two main issues here:

1. The representation of a physical state depends on which inner product we choose. Since there is no canonical way to pick the eigenvectors of a Hamiltonian, the inner product defined in [68] is not well-suited for comparing the physics of different systems, such as a family of Hamiltonians depending on some parameter, with each other.

2. Even if we do have a well-defined inner product, the interpretation of the

vectors $|e_n\rangle$ remains unclear. According to the biorthogonal formalism, they should represent different physical states when the inner product is changed and do not have an independent physical meaning, but as we have seen in Sec. 3.1 and as can be seen in experimental verifications of the biorthogonal bulk-boundary correspondence [35], these vectors *do* correspond to physical quantities.

These issues are addressed in Paper V, where we define an inner product that is independent of the choice of eigenvectors of the Hamiltonian. There, we avoid the associated state and instead define the inner product via an inner product matrix, G, which we define as

$$G = \sum_n \frac{\langle R_n | R_n \rangle}{|\langle L_n | R_n \rangle|^2} |L_n\rangle \langle L_n| , \tag{4.47}$$

such that the inner product of two states $|\alpha\rangle$ and $|\beta\rangle$ is given by

$$(|\alpha\rangle , |\beta\rangle)_G = \langle \alpha | G | \beta \rangle . \tag{4.48}$$

We see that rescaling the eigenstates of the Hamiltonian leaves G, and thus also the inner product, invariant. This means that the inner product is uniquely defined given a Hamiltonian, and thus comparisons between different systems are significantly simplified. We do, however, also show that there is no way to keep the meaning of the vectors $|e_n\rangle$ as positions in a lattice within the biorthogonal formalism. The conclusion from this is that even though the biorthogonal bulk-boundary correspondence is experimentally verified in several classical systems, the rest of the biorthogonal formalism is not straightforwardly mapped to a classical lattice model.

Chapter 5

Discussion and outlook

In this thesis, we have investigated what happens to the bulk-boundary correspondence in non-Hermitian systems. We have seen that the bulk-boundary correspondence known from the Hermitian case breaks down in the non-Hermitian realm. To understand what is going on in the non-Hermitian case, we study several systems in which we can find analytical expressions for the eigenvectors corresponding to a zero eigenvalue, and show that we can predict the gap closings by computing the biorthogonal expectation value of the operator $|e_n\rangle\langle e_n|$. We call this the *biorthogonal* bulk-boundary correspondence since the gaps in the spectrum of the system with open boundary conditions predict the (dis)appearance of biorthogonal boundary states. We show that this works out in several systems, both in the one-dimensional and the higher-dimensional case. The biorthogonal bulk-boundary correspondence is supported by experiments in the classical regime [35], where they make use of the fact that the system can be mapped to a Schrödinger-like equation. Previously, this method has been used to create a mapping between Hermitian Hamiltonians and classical systems, which then allows us to map physical properties of condensed matter systems to classical systems. In the non-Hermitian case, however, we argue that even though this map exists mathematically between these systems, it might not be possible to map the actual physical properties. In particular, we have seen that while the vector $|e_n\rangle$ has a physical meaning in a classical system, it might not have that in a biorthogonal quantum system, where it seems that the lattice model obtained from a non-Hermitian model might be more of a tool for visualization than of the existence of an actual physical system. This is certainly very interesting and should be investigated further.

The claim that $|e_n\rangle$ does not have a physical meaning in a biorthogonal quantum system, relies on the fact that the vector itself cannot be connected to a physical state without reference to an inner product. And since the inner product changes when we change the Hamiltonian, the physical meaning of the vector $|e_n\rangle$ would

also change. However, we have seen that computing the biorthogonal expectation value of the operator Π_n does predict something about the system and it would be very interesting to understand this better in a quantum setting. Is it even possible to realize such quantum systems?

Going back to the biorthogonal bulk-boundary correspondence, we note that this is an attempt to generalize the Hermitian bulk-boundary correspondence. In the Hermitian case, the bulk-boundary correspondence also includes the existence of a topological invariant that predicts the number of topological boundary states. In principle, there can be states localized at the boundary that are not topological, which means that the existence of an invariant is an important component of the bulk-boundary correspondence. In the non-Hermitian case there have been attempts to find invariants for the systems we have studied, but none of them have been as successful as in the Hermitian case. Examples include the work in [93] and [106]. We therefore note that the biorthogonal bulk-boundary correspondence is not a claim about topological properties of a system, but rather a connection between existence of boundary states and prediction of gap closings. This is still very important as the boundary states themselves and the gap closings give a lot of information about the system and also give a very strong hint towards where to look for topological invariants. It is tempting to say that it seems unlikely that a number computed from the Bloch Hamiltonian could say anything about the existence of topological boundary states in the system with open boundary conditions, but since the spectral winding number in Eq. (3.12) is computed from the Bloch Hamiltonian and still can predict the existence of the skin effect, we cannot rule out that something similar can be done for the boundary states. This would add additional robustness to the boundary states we have found.

As has been pointed out in the thesis, Papers I-III are focused on developing the biorthogonal bulk-boundary correspondence. This is done by studying several different systems, but we have not proven that the bulk-boundary correspondence exists in this form in general. This is an open question that would be important to study further. Mathematically, much is known about Toeplitz matrices (see e.g. [107]), but block-Toeplitz matrices are much harder to diagonalize. Trying to prove such a bulk-boundary correspondence might thus be challenging in more than one dimension.

That higher-dimensional systems are harder to understand is something we also see in Paper IV. In general, two-dimensional systems with open boundary conditions are not possible to diagonalize analytically. This makes it very hard to find conditions on the parameter values in the system for which we do not have a skin effect. As we demonstrate in Paper IV, it is not enough to balance a two-dimensional system in the two different directions separately; it seems to work if

the lattice has a square geometry, but when the lattice is rectangular the eigenstates start to localize even though balancing conditions are implemented in both directions. An example of this would be the triangular lattice. This is quite unintuitive, and having a better physical understanding of why this happens and what it means is desirable. The same goes for the fact that we cannot seem to balance hoppings of different lengths with one another, even though the naive thought would be that it should be possible.

Finally, a comment on experiments. Even though we study lattice models and this brings the thought to condensed matter systems, none of the experimental realizations are, to date, in that field. Most of them are classical and makes use of the fact that e.g. the equations of motion of some mechanical systems can be mapped to a Schrödinger-like equation with a non-Hermitian Hamiltonian. In the quantum regime there have been less experiments. In general, it is clear that even if it were possible to design a condensed matter system consisting of a non-Hermitian lattice, it could be very hard to actually construct such a system with open boundary conditions in reality since the skin effect makes such systems extremely sensitive to perturbations. On the other hand, the extreme sensitivity can also have advantages. One example of this is in sensors, something that has been discussed in [108, 109], where the suggestion is to construct quantum non-Hermitian topological sensors.

Bibliography

[1] E. Edvardsson, *Bulk-boundary correspodence in non-Hermitian systems*, Licentiate thesis, Stockholm university (2020).

[2] K. v. Klitzing, G. Dorda, and M. Pepper, New Method for High-Accuracy Determination of the Fine-Structure Constant Based on Quantized Hall Resistance, Phys. Rev. Lett. **45**, 494 (1980).

[3] C. L. Kane and E. J. Mele, Z_2 Topological Order and the Quantum Spin Hall Effect, Phys. Rev. Lett. **95**, 146802 (2005).

[4] C. L. Kane and E. J. Mele, Quantum Spin Hall Effect in Graphene, Phys. Rev. Lett. **95**, 226801 (2005).

[5] F. D. M. Haldane, Model for a Quantum Hall Effect without Landau Levels: Condensed-Matter Realization of the "Parity Anomaly", Phys. Rev. Lett. **61**, 2015 (1988).

[6] C.-Z. Chang, J. Zhang, X. Feng, J. Shen, Z. Zhang, M. Guo, K. Li, Y. Ou, P. Wei, L.-L. Wang, Z.-Q. Ji, Y. Feng, S. Ji, X. Chen, J. Jia, X. Dai, Z. Fang, S.-C. Zhang, K. He, Y. Wang, L. Lu, X.-C. Ma, and Q.-K. Xue, Experimental Observation of the Quantum Anomalous Hall Effect in a Magnetic Topological Insulator, Science **340**, 167 (2013).

[7] G. Jotzu, M. Messer, R. Desbuquois, M. Lebrat, T. Uehlinger, D. Greif, and T. Esslinger, Experimental realization of the topological Haldane model with ultracold fermions, Nature **515**, 237 (2014).

[8] M. König, S. Wiedmann, C. Brüne, A. Roth, H. Buhmann, L. W. Molenkamp, X.-L. Qi, and S.-C. Zhang, Quantum Spin Hall Insulator State in HgTe Quantum Wells, Science **318**, 766 (2007).

[9] B. A. Bernevig, T. L. Hughes, and S.-C. Zhang, Quantum Spin Hall Effect and Topological Phase Transition in HgTe Quantum Wells, Science **314**, 1757 (2006).

[10] B. A. Bernevig and S.-C. Zhang, Quantum Spin Hall Effect, Phys. Rev. Lett. **96**, 106802 (2006).

[11] F. Schindler, A. M. Cook, M. G. Vergniory, Z. Wang, S. S. P. Parkin, B. A. Bernevig, and T. Neupert, Higher-order topological insulators, Science Advances **4**, 10.1126/sciadv.aat0346 (2018).

[12] W. A. Benalcazar, B. A. Bernevig, and T. L. Hughes, Quantized electric multipole insulators, Science **357**, 61 (2017).

[13] W. A. Benalcazar, B. A. Bernevig, and T. L. Hughes, Electric multipole moments, topological multipole moment pumping, and chiral hinge states in crystalline insulators, Phys. Rev. B **96**, 245115 (2017).

[14] Z. Song, Z. Fang, and C. Fang, $(d-2)$-Dimensional Edge States of Rotation Symmetry Protected Topological States, Phys. Rev. Lett. **119**, 246402 (2017).

[15] J. Langbehn, Y. Peng, L. Trifunovic, F. von Oppen, and P. W. Brouwer, Reflection-Symmetric Second-Order Topological Insulators and Superconductors, Phys. Rev. Lett. **119**, 246401 (2017).

[16] A. Szameit, M. C. Rechtsman, O. Bahat-Treidel, and M. Segev, $\mathcal{PT}$-symmetry in honeycomb photonic lattices, Phys. Rev. A **84**, 021806 (2011).

[17] A. Regensburger, C. Bersch, M.-A. Miri, G. Onishchukov, D. N. Christodoulides, and U. Peschel, Parity–time synthetic photonic lattices, Nature **488**, 167 (2012).

[18] J. Wiersig, Enhancing the Sensitivity of Frequency and Energy Splitting Detection by Using Exceptional Points: Application to Microcavity Sensors for Single-Particle Detection, Phys. Rev. Lett. **112**, 203901 (2014).

[19] G. Harari, M. A. Bandres, Y. Lumer, M. C. Rechtsman, Y. D. Chong, M. Khajavikhan, D. N. Christodoulides, and M. Segev, Topological insulator laser: Theory, Science **359**, 10.1126/science.aar4003 (2018).

[20] M. A. Bandres, S. Wittek, G. Harari, M. Parto, J. Ren, M. Segev, D. N. Christodoulides, and M. Khajavikhan, Topological insulator laser: Experiments, Science **359**, 10.1126/science.aar4005 (2018).

[21] H. Hodaei, A. U. Hassan, S. Wittek, H. Garcia-Gracia, R. El-Ganainy, D. N. Christodoulides, and M. Khajavikhan, Enhanced sensitivity at higher-order exceptional points, Nature **548**, 187 (2017).

[22] L. Feng, R. El-Ganainy, and L. Ge, Non-Hermitian photonics based on parity–time symmetry, Nature Photonics **11**, 752 (2017).

[23] D. L. Sounas and A. Alù, Non-reciprocal photonics based on time modulation, Nature Photonics **11**, 774 (2017).

[24] H. Zhao, P. Miao, M. H. Teimourpour, S. Malzard, R. El-Ganainy, H. Schomerus, and L. Feng, Topological hybrid silicon microlasers, Nature communications **9**, 1 (2018).

[25] M. Kremer, T. Biesenthal, L. J. Maczewsky, M. Heinrich, R. Thomale, and A. Szameit, Demonstration of a two-dimensional PT-symmetric crystal, Nature communications **10**, 1 (2019).

[26] Ş. Özdemir, S. Rotter, F. Nori, and L. Yang, Parity–time symmetry and exceptional points in photonics, Nature materials **18**, 783 (2019).

[27] J. Ningyuan, C. Owens, A. Sommer, D. Schuster, and J. Simon, Time- and Site-Resolved Dynamics in a Topological Circuit, Phys. Rev. X **5**, 021031 (2015).

[28] V. V. Albert, L. I. Glazman, and L. Jiang, Topological Properties of Linear Circuit Lattices, Phys. Rev. Lett. **114**, 173902 (2015).

[29] M. Ezawa, Non-Hermitian higher-order topological states in nonreciprocal and reciprocal systems with their electric-circuit realization, Phys. Rev. B **99**, 201411 (2019).

[30] T. Helbig, T. Hofmann, S. Imhof, M. Abdelghany, T. Kiessling, L. Molenkamp, C. Lee, A. Szameit, M. Greiter, and R. Thomale, Generalized bulk–boundary correspondence in non-Hermitian topolectrical circuits, Nature Physics **16**, 747 (2020).

[31] T. Hofmann, T. Helbig, F. Schindler, N. Salgo, M. Brzezińska, M. Greiter, T. Kiessling, D. Wolf, A. Vollhardt, A. Kabaši, *et al.*, Reciprocal skin effect and its realization in a topolectrical circuit, Physical Review Research **2**, 023265 (2020).

[32] C. H. Lee, S. Imhof, C. Berger, F. Bayer, J. Brehm, L. W. Molenkamp, T. Kiessling, and R. Thomale, Topolectrical circuits, Communications Physics **1**, 1 (2018).

[33] L. M. Nash, D. Kleckner, A. Read, V. Vitelli, A. M. Turner, and W. T. M. Irvine, Topological mechanics of gyroscopic metamaterials, Proceedings of the National Academy of Sciences **112**, 14495 (2015).

[34] M. Brandenbourger, X. Locsin, E. Lerner, and C. Coulais, Non-reciprocal robotic metamaterials, Nature communications **10**, 1 (2019).

[35] A. Ghatak, M. Brandenbourger, J. Van Wezel, and C. Coulais, Observation of non-Hermitian topology and its bulk–edge correspondence in an active mechanical metamaterial, Proceedings of the National Academy of Sciences **117**, 29561 (2020).

[36] K. Kawabata, T. Bessho, and M. Sato, Classification of Exceptional Points and Non-Hermitian Topological Semimetals, Phys. Rev. Lett. **123**, 066405 (2019).

[37] C. H. Lee, L. Li, and J. Gong, Hybrid Higher-Order Skin-Topological Modes in Nonreciprocal Systems, Phys. Rev. Lett. **123**, 016805 (2019).

[38] J. Carlström, M. Stålhammar, J. C. Budich, and E. J. Bergholtz, Knotted non-Hermitian metals, Phys. Rev. B **99**, 161115 (2019).

[39] J. C. Budich, J. Carlström, F. K. Kunst, and E. J. Bergholtz, Symmetry-protected nodal phases in non-Hermitian systems, Phys. Rev. B **99**, 041406 (2019).

[40] H. Zhou and J. Y. Lee, Periodic table for topological bands with non-Hermitian symmetries, Phys. Rev. B **99**, 235112 (2019).

[41] M. Stålhammar, L. Rødland, G. Arone, J. C. Budich, and E. J. Bergholtz, Hyperbolic Nodal Band Structures and Knot Invariants, SciPost Phys. **7**, 19 (2019).

[42] H. Shen, B. Zhen, and L. Fu, Topological band theory for non-Hermitian Hamiltonians, Physical review letters **120**, 146402 (2018).

[43] K. Kawabata, K. Shiozaki, M. Ueda, and M. Sato, Symmetry and Topology in Non-Hermitian Physics, Phys. Rev. X **9**, 041015 (2019).

[44] K. Esaki, M. Sato, K. Hasebe, and M. Kohmoto, Edge states and topological phases in non-Hermitian systems, Phys. Rev. B **84**, 205128 (2011).

[45] J. Carlström and E. J. Bergholtz, Exceptional links and twisted Fermi ribbons in non-Hermitian systems, Phys. Rev. A **98**, 042114 (2018).

[46] Z. Gong, Y. Ashida, K. Kawabata, K. Takasan, S. Higashikawa, and M. Ueda, Topological Phases of Non-Hermitian Systems, Phys. Rev. X **8**, 031079 (2018).

[47] D. Leykam, K. Y. Bliokh, C. Huang, Y. D. Chong, and F. Nori, Edge Modes, Degeneracies, and Topological Numbers in Non-Hermitian Systems, Phys. Rev. Lett. **118**, 040401 (2017).

[48] D. J. Luitz and F. Piazza, Exceptional points and the topology of quantum many-body spectra, Phys. Rev. Research **1**, 033051 (2019).

[49] X.-W. Luo and C. Zhang, Higher-Order Topological Corner States Induced by Gain and Loss, Phys. Rev. Lett. **123**, 073601 (2019).

[50] C. Poli, M. Bellec, U. Kuhl, F. Mortessagne, and H. Schomerus, Selective enhancement of topologically induced interface states in a dielectric resonator chain, Nature communications **6**, 1 (2015).

[51] H. Zhou, J. Y. Lee, S. Liu, and B. Zhen, Exceptional surfaces in PT-symmetric non-hermitian photonic systems, Optica **6**, 190 (2019).

[52] H. Zhou, C. Peng, Y. Yoon, C. W. Hsu, K. A. Nelson, L. Fu, J. D. Joannopoulos, M. Soljačić, and B. Zhen, Observation of bulk Fermi arc and polarization half charge from paired exceptional points, Science **359**, 1009 (2018).

[53] H. He, C. Qiu, L. Ye, X. Cai, X. Fan, M. Ke, F. Zhang, and Z. Liu, Topological negative refraction of surface acoustic waves in a Weyl phononic crystal, Nature **560**, 61 (2018).

[54] L. Xiao, T. Deng, K. Wang, G. Zhu, Z. Wang, W. Yi, and P. Xue, Non-Hermitian bulk–boundary correspondence in quantum dynamics, Nature Physics **16**, 761 (2020).

[55] A. Cerjan, S. Huang, M. Wang, K. P. Chen, Y. Chong, and M. C. Rechtsman, Experimental realization of a Weyl exceptional ring, Nature Photonics **13**, 623 (2019).

[56] W. Chen, Ş. K. Özdemir, G. Zhao, J. Wiersig, and L. Yang, Exceptional points enhance sensing in an optical microcavity, Nature **548**, 192 (2017).

[57] S. Weimann, M. Kremer, Y. Plotnik, Y. Lumer, S. Nolte, K. G. Makris, M. Segev, M. C. Rechtsman, and A. Szameit, Topologically protected bound states in photonic parity–time-symmetric crystals, Nature materials **16**, 433 (2017).

[58] B. Peng, Ş. K. Özdemir, M. Liertzer, W. Chen, J. Kramer, H. Yılmaz, J. Wiersig, S. Rotter, and L. Yang, Chiral modes and directional lasing at exceptional points, Proceedings of the National Academy of Sciences **113**, 6845 (2016).

[59] J. M. Zeuner, M. C. Rechtsman, Y. Plotnik, Y. Lumer, S. Nolte, M. S. Rudner, M. Segev, and A. Szameit, Observation of a Topological Transition in the Bulk of a Non-Hermitian System, Phys. Rev. Lett. **115**, 040402 (2015).

[60] Z. Wang, Y. Chong, J. D. Joannopoulos, and M. Soljačić, Observation of unidirectional backscattering-immune topological electromagnetic states, Nature **461**, 772 (2009).

[61] Y. Xiong, T. Wang, X. Wang, and P. Tong, Comment on" Anomalous Edge State in a Non-Hermitian Lattice", arXiv preprint arXiv:1610.06275 (2016).

[62] T. E. Lee, Anomalous Edge State in a Non-Hermitian Lattice, Phys. Rev. Lett. **116**, 133903 (2016).

[63] Y. Xiong, Why does bulk boundary correspondence fail in some non-hermitian topological models, Journal of Physics Communications **2**, 035043 (2018).

[64] V. M. Martinez Alvarez, J. E. Barrios Vargas, and L. E. F. Foa Torres, Non-Hermitian robust edge states in one dimension: Anomalous localization and eigenspace condensation at exceptional points, Phys. Rev. B **97**, 121401 (2018).

[65] F. K. Kunst, G. van Miert, and E. J. Bergholtz, Lattice models with exactly solvable topological hinge and corner states, Phys. Rev. B **97**, 241405 (2018).

[66] F. K. Kunst, M. Trescher, and E. J. Bergholtz, Anatomy of topological surface states: Exact solutions from destructive interference on frustrated lattices, Phys. Rev. B **96**, 085443 (2017).

[67] F. K. Kunst, G. van Miert, and E. J. Bergholtz, Boundaries of boundaries: A systematic approach to lattice models with solvable boundary states of arbitrary codimension, Physical Review B **99**, 085426 (2019).

[68] D. C. Brody, Biorthogonal quantum mechanics, Journal of Physics A: Mathematical and Theoretical **47**, 035305 (2013).

[69] F. K. Kunst, E. Edvardsson, J. C. Budich, and E. J. Bergholtz, Biorthogonal Bulk-Boundary Correspondence in Non-Hermitian Systems, Phys. Rev. Lett. **121**, 026808 (2018).

[70] E. Edvardsson, F. K. Kunst, and E. J. Bergholtz, Non-Hermitian extensions of higher-order topological phases and their biorthogonal bulk-boundary correspondence, Phys. Rev. B **99**, 081302 (2019).

[71] E. Edvardsson, T. Yoshida, F. K. Kunst, and E. J. Bergholtz, Phase Transitions and Generalized Trace Polarization in non-Hermitian systems (2020), in preparation.

[72] E. Edvardsson and E. Ardonne, Sensitivity of non-Hermitian systems, Physical Review B **106**, 115107 (2022).

[73] E. Edvardsson, J. L. K. König, and M. Stålhammar, Biorthogonal renormalization (2022), manuscript.

[74] J. M. Lee, *Introduction to Topological Manifolds*, 2nd ed. (Springer, 2011).

[75] B. A. Bernevig and T. L. Hughes, *Topological insulators and topological superconductors* (Princeton university press, 2013).

[76] A. Altland and M. R. Zirnbauer, Nonstandard symmetry classes in mesoscopic normal-superconducting hybrid structures, Phys. Rev. B **55**, 1142 (1997).

[77] S. Ryu, A. P. Schnyder, A. Furusaki, and A. W. Ludwig, Topological insulators and superconductors: tenfold way and dimensional hierarchy, New Journal of Physics **12**, 065010 (2010).

[78] G. Stewart and J. Sun, *Matrix Perturbation Theory*, Computer Science and Scientific Computing (Elsevier Science, 1990).

[79] W. P. Su, J. R. Schrieffer, and A. J. Heeger, Solitons in Polyacetylene, Phys. Rev. Lett. **42**, 1698 (1979).

[80] W. P. Su, J. R. Schrieffer, and A. J. Heeger, Soliton excitations in polyacetylene, Phys. Rev. B **22**, 2099 (1980).

[81] J. K. Asbóth, L. Oroszlány, and A. Pályi, *A short course on topological insulators*, Vol. 919 (Springer, 2016) p. 87.

[82] S. Ryu and Y. Hatsugai, Topological origin of zero-energy edge states in particle-hole symmetric systems, Physical review letters **89**, 077002 (2002).

[83] S. A. Parameswaran and Y. Wan, Topological insulators turn a corner, Physics **10**, 132 (2017).

[84] F. K. Kunst, G. van Miert, and E. J. Bergholtz, Extended Bloch theorem for topological lattice models with open boundaries, Phys. Rev. B **99**, 085427 (2019).

[85] C. M. Bender, Introduction to PT-symmetric quantum theory, Contemporary Physics **46**, 277 (2005), https://doi.org/10.1080/00107500072632 .

[86] C. M. Bender, Making sense of non-Hermitian Hamiltonians, Reports on Progress in Physics **70**, 947 (2007).

[87] C. M. Bender and S. Boettcher, Real Spectra in Non-Hermitian Hamiltonians Having PT Symmetry, Phys. Rev. Lett. **80**, 5243 (1998).

[88] R. El-Ganainy, K. G. Makris, M. Khajavikhan, Z. H. Musslimani, S. Rotter, and D. N. Christodoulides, Non-Hermitian physics and PT symmetry, Nature Physics **14**, 11 (2018).

[89] T. Yoshida and Y. Hatsugai, Exceptional rings protected by emergent symmetry for mechanical systems, Phys. Rev. B **100**, 054109 (2019).

[90] G. Lindblad, On the generators of quantum dynamical semigroups, Communications in Mathematical Physics **48**, 119 (1976).

[91] F. Song, S. Yao, and Z. Wang, Non-Hermitian skin effect and chiral damping in open quantum systems, Physical review letters **123**, 170401 (2019).

[92] F. Yang, Q.-D. Jiang, and E. J. Bergholtz, Liouvillian skin effect in an exactly solvable model, Physical Review Research **4**, 023160 (2022).

[93] S. Yao and Z. Wang, Edge states and topological invariants of non-Hermitian systems, Physical review letters **121**, 086803 (2018).

[94] W. Heiss, The physics of exceptional points, Journal of Physics A: Mathematical and Theoretical **45**, 444016 (2012).

[95] A. Guo, G. Salamo, D. Duchesne, R. Morandotti, M. Volatier-Ravat, V. Aimez, G. Siviloglou, and D. Christodoulides, Observation of P T-symmetry breaking in complex optical potentials, Physical Review Letters **103**, 093902 (2009).

[96] S. Lieu, Topological phases in the non-Hermitian Su-Schrieffer-Heeger model, Physical Review B **97**, 045106 (2018).

[97] D. Braghini, L. G. Villani, M. I. Rosa, and J. R. de F Arruda, Non-Hermitian elastic waveguides with piezoelectric feedback actuation: non-reciprocal bands and skin modes, Journal of Physics D: Applied Physics **54**, 285302 (2021).

[98] Q. Liang, D. Xie, Z. Dong, H. Li, H. Li, B. Gadway, W. Yi, and B. Yan, Dynamic Signatures of Non-Hermitian Skin Effect and Topology in Ultracold Atoms, Phys. Rev. Lett. **129**, 070401 (2022).

[99] N. Okuma, K. Kawabata, K. Shiozaki, and M. Sato, Topological Origin of Non-Hermitian Skin Effects, Phys. Rev. Lett. **124**, 086801 (2020).

[100] K. Zhang, Z. Yang, and C. Fang, Universal non-Hermitian skin effect in two and higher dimensions, Nature communications **13**, 1 (2022).

[101] D. C. Brody, Consistency of PT-symmetric quantum mechanics, Journal of Physics A: Mathematical and Theoretical **49**, 10LT03 (2016).

[102] M. J. Rice and E. J. Mele, Elementary Excitations of a Linearly Conjugated Diatomic Polymer, Phys. Rev. Lett. **49**, 1455 (1982).

[103] H. Schomerus, Nonreciprocal response theory of non-Hermitian mechanical metamaterials: Response phase transition from the skin effect of zero modes, Phys. Rev. Research **2**, 013058 (2020).

[104] M. Znojil, On the Role of the Normalization Factors κ_n and of the Pseudo-Metric P$\neq$ P$\hat{}\dagger$ in Crypto-Hermitian Quantum Models, SIGMA. Symmetry, Integrability and Geometry: Methods and Applications **4**, 001 (2008).

[105] A. Leclerc, D. Viennot, and G. Jolicard, The role of the geometric phases in adiabatic population tracking for non-Hermitian Hamiltonians, Journal of Physics A: Mathematical and Theoretical **45**, 415201 (2012).

[106] C. Yin, H. Jiang, L. Li, R. Lü, and S. Chen, Geometrical meaning of winding number and its characterization of topological phases in one-dimensional chiral non-Hermitian systems, Physical Review A **97**, 052115 (2018).

[107] A. Böttcher and S. M. Grudsky, *Spectral properties of banded Toeplitz matrices* (SIAM, 2005).

[108] J. C. Budich and E. J. Bergholtz, Non-Hermitian Topological Sensors, Phys. Rev. Lett. **125**, 180403 (2020).

[109] F. Koch and J. C. Budich, Quantum non-Hermitian topological sensors, Phys. Rev. Research **4**, 013113 (2022).